NTNU – Trondheim
Norwegian University of
Science and Technology

Parameter study of electric power production in wind farms - experiments using two model scale wind turbines

Szymon Luczynski

Master's Thesis
Submission date: December 2014
Supervisor: Lars Sætran, EPT
Co-supervisor: Piotr Domagalski, Lodz University of Technology

Norwegian University of Science and Technology
Department of Energy and Process Engineering

NTNU

Norwegian University
of Science and Technology

Department of Energy
and Process Engineering

EPT-M-2014-139

MASTER THESIS

for

Szymon Luczynski

Spring 2014

Parameter study of electric power production in wind farms –experiments using two model scale wind turbines

Parameterstudie av elektrisk effekt-produksjon i vindparker –eksperimenter hvor det benyttes to modellskala vindturbiner

Background and objective

The maximum power rating of wind turbines (WTs) is nowadays around 5 - 8 MW. The current value of rated power of individual WTs, along with the increase in the capacity of the wind power plants (especially in the case of offshore facilities) requires the installation of a large number of turbines in a relatively small area: a 1 GW wind farm (WF) would need 200 WTs of 5 MW. Under these circumstances, the wake effect plays a key role when evaluating the energy production of a WF, since the energy captured by a WT leads to a decrease of the wind speed downstream. As a result, WTs located downstream produce less energy than if they were in air free-flow. In the case of onshore WFs, the energy losses due to the wake effect constitute about 5 - 10% of the production [1], while in offshore WFs, the wake effect losses can reach higher values; approximately 15% [2]. This increase results from the higher degree of compactness (number of turbines per unit area) of offshore wind farms due to their high implementation costs. During the design stage of a wind farm, and in order to increase the WF production (by reducing wind speed deficits or wake effect losses), it would be desirable to separate the WTs as far as possible. However, due to constraints such as surface availability and cost of electrical connections and the total cost of electrical losses over the lifespan of the installation [3], [4], the maximum distance between WTs is limited. Consequently, the general rule when deciding the layout of WTs is to locate the WTs as far away from each other as possible according to the prevailing wind directions. However, not even in the case of prevailing wind directions it is possible to completely prevent wake-effect losses. Furthermore, these wake losses are higher for the remaining wind directions due to the shorter distance between WTs according to these directions. Although the power production of the wind farm for non-prevailing wind directions is less, its frequency means that the annual amount of energy generated for these wind directions remains significant.

The usual operating mode of each WT in a wind farm is to set the pitch angle and the tip speed ratio so that the WT strives to capture the n dynamic power available from the air

inflow at the position of each WT. This means that every WT operates with the maximum power coefficient when the wind speed is lower than the rated wind speed, or operates at rated power for higher wind speeds. However, in a WT cluster, this operating mode is not optimum in terms of the overall production (aerodynamic efficiency) of the WF, because the energy captured by each WT decreases the aerodynamic power available to other downwind turbines due the wake effect. Therefore, it might be possible to find an optimal operation strategy by individually controlling the setup of each WT so that the overall wake effect losses (speed deficits) are minimized and, as a consequence, the power production of the plant is maximized.

The concept of individual control power of WTs was initially suggested by Steinbuch et al. [5] by selecting the tip speed ratio of each wind turbine by means of trial and error. However, according to the conclusion presented by the authors, the increase in the output power obtained by this method was insignificant. In 2004, Corten and Schaak [6] presented experimental results showing the possibility of increasing the power generated and of reducing the loads by individually selecting the tip speed ratio of each wind turbine. In early 2011, Larsen et al. [7] presented the technical report corresponding to the TOPFARM project which deals with optimal topology design and control of wind farms. That study showed that it is possible to increase the overall efficiency of a WF through the individual control of the generated power by each WT, however no further details are provided on how this control can be implemented or what the degree of the production improvement would be. In 2011, Madjidian and Rantzer [8] proposed the control of the power generated by the WTs in order to increase the overall efficiency corresponding to a row of wind turbines. With the purpose of evaluating the wake effect, the authors suggested a recursive model dependent on the thrust coefficient of the WTs. Through this wake model, the authors proposed a global control of the wind farm by using the same set point for all WTs. In 2012, Lee et al. [9] , presented a strategy of individual control of each of the WTs by optimizing the pitch angle of each turbine by means of a genetic algorithm, and used a wake model based on the eddy viscosity model. In that study, the authors considered the case of a row of wind turbines and achieved an improvement in the aerodynamic power of 4.5% with regard to the conventional operating strategy (COS).

The following tasks are to be considered:

For the development of theoretical simulation models for control of individual WTs in a WF it is necessary to calibrate the model with experimental results of good quality. For full-scale WFs there is difficult to find documented experimental cases where all necessary parameters are controlled and measured. Therefore, one can use model scale experiments as benchmark cases. For this work we propose to do experiments using the wind tunnel and the 2 model WTs at the EPT department. The main goal is to find criteria for optimum total power production for this "2-WT-WF". Parameters to be varied can be: Tip Speed Ratio for both WTs, separation distance between the WTs, turbulence level in the incoming wind, shear in the incoming wind, yaw angle of the WTs, pitch angle of the rotor blades, etc.

This is an ongoing research program at our department [10], [11], [12], and the student is supposed to both work in a team with other students and to do individual experiments. The experimental results obtained will be part of a data bank, and the student will choose parameters and results that shall be analyzed in detail.

References:

[1] Krohn S., Morthorst P.E. and Awerbuch S. The economics of wind energy. European Wind Energy Available: http://www.ewea.org/fileadmin/ewea_documents/documents/00_POLICY_document/Economics_of_Wind_Energy__March_2009_.pdf; March 2009 [accessed 08.05.11].
[2] Barthelmie R., Larsen G., Frandsen S., Folkerts L., Rados K., Pryor S., Lange B. and Schepers G., Comparison of wake model simulations with offshore wind turbine wake profiles measured by SODAR, J.Atmos.Ocean.Technol.,

2006; 23(7): 888-901.
[3] Serrano González J., González Rodríguez Á.G., Castro Mora J., Burgos Payán M., Riquelme Santos J., Overall design optimization of wind farms, RenewableEnergy. 2011;36: 1973-1982.
[4] Serrano González J., Burgos Payán M., Riquelme Santos J., Optimum design of transmissions systems for offshore wind farms including decision making under risk, Renewable Energy. 2013; 59: 115-127.
[5] Steinbuch M., de Boer W., Bosgra O., Peters S., Ploeg J., Optimal control of wind power plants, J. Wind Eng. Ind. Aerodyn. 1988; 27: 237-246.
[6] Corten G., Schaak P. and Bot E., More Power and Less Loads in Wind Farms:'Heat and Flux', In: European Wind Energy Conference & Exhibition, 2004, London.
[7] Larsen GC, Aagaard Madsen H, Troldborg N, Larsen TJ, Réthoré P, Fuglsang P et al. TOPFARM-next generation design tool for optimisation of wind farm topology and operation. 2011.
[8] Madjidian D. and Rantzer, A. A stationary turbine interaction model for control of wind farms, in IFAC 18th World Congress, 2011.
[9] Lee J., Son E., Hwang B. and Lee S., Blade pitch angle control for aerodynamic performance optimization of a wind farm, Renewable Energy. 2012; 54:124-130.
[10] Krogstad P-Å. and Eriksen P.E. "Blind test" calculations of the performance and wake development for a model wind turbine, Renewable Energy. 2013: 50: 325-333
[11] Pierella F, Krogstad P-Å. And Sætran L.R. Renewable Energy 2014: XX: 1-12
[12] Krogstad P-Å., Sætran L.R. and Adaramola S. J Fluids and Structure 2014 (accepted)

-- " --

Within 14 days of receiving the written text on the master thesis, the candidate shall submit a research plan for his project to the department.

When the thesis is evaluated, emphasis is put on processing of the results, and that they are presented in tabular and/or graphic form in a clear manner, and that they are analyzed carefully.

The thesis should be formulated as a research report with summary both in English and Norwegian, conclusion, literature references, table of contents etc. During the preparation of the text, the candidate should make an effort to produce a well-structured and easily readable report. In order to ease the evaluation of the thesis, it is important that the cross-references are correct. In the making of the report, strong emphasis should be placed on both a thorough discussion of the results and an orderly presentation.

The candidate is requested to initiate and keep close contact with his/her academic supervisor(s) throughout the working period. The candidate must follow the rules and regulations of NTNU as well as passive directions given by the Department of Energy and Process Engineering.

Risk assessment of the candidate's work shall be carried out according to the department's procedures. The risk assessment must be documented and included as part of the final report. Events related to the candidate's work adversely affecting the health, safety or security, must be documented and included as part of the final report. If the documentation on risk assessment represents a large number of pages, the full version is to be submitted electronically to the supervisor and an excerpt is included in the report.

Pursuant to "Regulations concerning the supplementary provisions to the technology study program/Master of Science" at NTNU §20, the Department reserves the permission to utilize all the results and data for teaching and research purposes as well as in future publications.

The final report is to be submitted digitally in DAIM. An executive summary of the thesis including title, student's name, supervisor's name, year, department name, and NTNU's logo and name, shall be submitted to the department as a separate pdf file. Based on an agreement with the

supervisor, the final report and other material and documents may be given to the supervisor in digital format.

☑ Work to be done in lab (Water power lab, Fluids engineering lab, Thermal engineering lab)
☐ Field work

Department of Energy and Process Engineering, 14. August 2014

Olav Bolland
Department Head

Lars Sætran
Academic Supervisor

Research Advisor: Jan Bartl

Acknowledgements

Considering complexity and amount of experiments results shown in this thesis it was made in cooperation with team of students which I would like to acknowledge my gratitude for time, help and patience with measurements. Without those people those experiments would be impossible to finish on time. In alphabetical order:

- **Jan Bartl** – PhD candidate at Norwegian University of Science and Technology,
- **Clio Cecotti** – Master student at Universitá Politecnica delle Marche in Ancona (Italy),
- **Andrea Spiga** – Master student at Universitá Politecnica delle Marche in Ancona (Italy),
- **Piotr Wiklak** – PhD candidate at Lodz University of Technology (Poland).

I would like to thank my Norwegian supervisor Lars R. Sætran for his support in difficult moments of my work and also for his confidence that this project will be successful.

I would like to express my appreciate for Pål Egil Eriksen who led me through hot-wire anemometry course and was always helpful with encountered issues.

Finally, special acknowledgements to my co-supervisor in Poland Piotr Domagalski who every time gave me his support and believed in me. What is more he was responsible for arrangement whole exchange program between NTNU and LUT.

Preface

Following master thesis has been performed at Department of Energy and Process Engineering, Faculty of Engineering Science and Technology at Norwegian University of Science and Technology (NTNU) in Trondheim. This thesis will be submitted for the degree Master Science in Process Engineering at Lodz University of Technology in Poland.

Presented project was made as a 4th part of the series of experiments called “Blind Test” performed by Department of Energy and Process Engineering for last few years. The upcoming results will be used as a comparison with simulations and validation of models used in the design of wind farms. Final outcome of this research will be publication in the scientific journal.

Abstract

During the last years the growing amount of a wind turbines was observed, but limited area requires to build them closer to each other or group them in clusters called wind farms. Interactions between the turbines have primary influence on decrease of total power generated in the wind parks. To design a wind park, the sophisticated software, able to model and simulate aerodynamic processes is required. Such models however need experimental validation or at least some reference test cases, what is currently missing [26,29,30]. Current work is therefore an attempt to build part of such reference data for upgrading or evaluating turbine interaction modeling tools typically used for wind park design.

At this project two models of horizontal axis wind turbines were used with rotor diameter around 0.9 m. Measurements were performed at large, approximately 12 m^2 cross-section, wind tunnel at Norwegian University of Science and Technology (NTNU) in Trondheim.

The main aim of this project was to find the best conditions of total power production of the two in-line turbines where only TSR was varied. The second aim of the project was to investigate wind velocity and turbulence intensity development behind the first turbine of the wind farm – CTA anemometry with single HW probe was used. Moreover, there were few additional cases: income flow was characterized by low or high turbulence and separation distance of the turbines was changed (3D, 5D, 9D rotor diameters separation).

The study confirms that it is possible to find best optimal setup, different than designed to work in unobstructed flow. Depending on the type of inlet stream flow and separation distance the increase of total power production between 2.09% to 10.7% for the T_2 TSR varied between 4.0 – 5.0 was found. Behavior of the T_1 TSR was also varied but closer to designed value of TSR=6.0. The best combined power coefficient of both turbines of Cp_{total}=0.762 was found at 9D separation distance with high turbulent inlet stream.

Wake measurements confirmed behavior of power coefficient for different setups. The recovery of the velocity profile and decrease of turbulence intensity moving axially downstream was observed. Moreover, high turbulent inlet flow was characterized by smoother profiles of turbulence intensity and wind velocity, which caused faster recovery of the wake, than case with low turbulent inlet flow.

Table of contests

List of Figures

List of tables

List of symbols

Symbol	Definition
A	Rotor area [m^2]
a	Velocity ratio [-]
Cp	Power coefficient [-]
Cp_{total}	Combined power coefficient [-]
Ct	Thrust coefficient [-]
D	Wind turbine diameter [m]
g	Gravity [m/s^2]
m	Mass [kg]
N	Number of samples [-]
P	Power generated by wind turbine [W]
P_0	Power carried by the wind [W]
R	Wind turbine radius [m]
T	Thrust [N]
TI	Turbulence intensity [%]
TSR, λ	Tip-speed ratio [-]
U	Free stream velocity [m/s]
$\bar{U}$	Mean velocity [m/s]
u'_i	Fluctuating velocity [m/s]
α	Angle of attack [^{o}]
ρ	Density [kg/m^3]
ω	Angular velocity [rad/s]

1 Background

1.1 Wind energy development – past, current, future

Wind energy have been used by human for centuries. Its history begins in ancient Egypt 5,000 years ago, where ships with sails were used, through Babylon 2000 B.C., where we can find the first notes about usage of machines similar to modern propellers till the 10th century A.D., where in the area of today Iran and Afghanistan windmills had been known. The first windmills in Europe were known from the 12th century A.D and they were used to mill grain [1].

The first "wind turbine" producing electricity was windmill invented in 1888 by Charles F. Bush (Cleveland, Ohio) and since that time usage of wind turbines completely changed. Before and just after Ward War II there were several reasons to produce electric energy from the wind. First one was high prices of fossil fuels and second was big distance to electric grids but after that time wind energy was temporarily forgotten. [2]

Of course knowledge has been still developed and over the years pioneers invented new shapes of airfoils, new electric generators and also tested vertical and horizontal types of turbines. Real boom that wind turbines were improved and well developed started in early 80 of 20th century. Since that time size of constructed rotors and towers were increasing as well as power generated from this source [3].

Nowadays, rise of the energy production from wind is still observed. Each year more and more wind parks are built. In the end of 2013 world wind energy capacity reached 318 529 MW after 282 275 MW in 2012. World Wind Energy Association provides that global production of wind energy in 2020 reach 700 000 MW. [4] Constant growth during past years and future prediction of wind energy production is shown on Fig. 1.

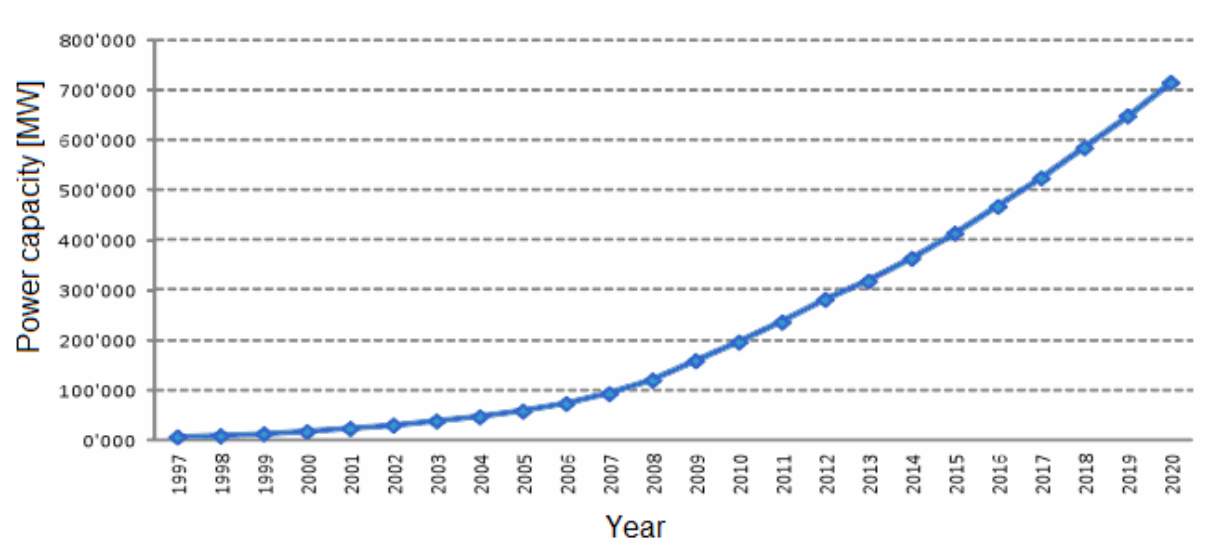

Fig. 1. Total installed capacity in 1997 – 2020 – development and prognosis [5]

There are many reasons why growth in power production from wind is observed. Firstly, reports from all around the world say that the fossil fuels are limited. There are not enough sources to give stability with the energy production in next 200 years [5]. Secondly, many of people believe that the Global Warming can be reduced or even stopped, when people reduce consumption of the energy or they use renewable energy sources. Third, the most important one for the European Union and countries in eastern part of the continent (also Poland), is the energetic instability and the dependence on Russian's Federation resources of fossil fuels. Current events in Ukraine and in Russia demonstrate even more that energy independence is very important. Therefore renewable energy could be one of directions for development of future energy sources, where wind energy is one of the most promising.

Good example worthy to copy is Denmark which is unrequested leader in wind power production. Already electric energy from wind has covered 34% of its demand and by 2020 Denmark plans to increase the share to 50%. To fulfill this project the capacity of wind farms have to increase by 1800 MW onshore, 500 MW near-shore and 1000MW offshore [6]. Other example of leading in wind resource utilization could be the Netherlands, which has ability to cover 100% of its electric needs in next 10 years. This idea is confirmed by serious simulations [7].

1.2 Current problems

As it was stated before, development of wind energy technology could be one of ways to improve capacity of the electric grid. There are a lot of ways to increase power generation from the wind.

One direction of development is that new wind power farms could become bigger and higher, but the area and durability of materials are limited. Also investment costs will increase with growth of the turbines size. What is more, expenditures only for space would be higher because turbines cannot stand next to each other. Next turbine in the same alignment will be affected by upstream turbine and will produce less power than working alone. The affection is named wake. The wake is common term in the fluid dynamics used to characterize part of the flow field behind objects with lower velocity and higher turbulence intensity than in main stream.

Right now the distance between each turbine in typical wind park, where downstream turbine works with similar efficiency to upstream, is estimated to be around 10 rotor diameters [8]. In such space arrangement the velocity defects are almost unnoticeable, but in modern wind parks turbines are situated much closer, which means higher influence between turbines. [9,10,11] Smaller separation is caused by rough optimization of investment and operational costs.

Interactions between turbines in wind farms are complex and still hard to predict by Computational Fluid Dynamics (CFD). For instance, modeling at the same time, flow over the turbine blades and the flow of the near and far wake has to be computed. It means that serious computer resources are needed due to the unsteady and turbulent character of the flow. Moreover, modelers feces problems connected with computational mesh generation [12]. To improve the wind park design efficiency and precision the reliable modeling tools and techniques are needed, taking into consideration different behavior of turbines operating in full and semi wake zone. Numerical predictions should be connected as well with power and thrust behavior as with wake and turbulence intensity. Therefore it was decided to prepare data bank of various performance setup of two in-line turbines serving as a set of test cases for development and evaluation of wind farm design tools and numerical models. That was realized as a series of closed wind tunnel tests with two scale model turbines.

2 Scope of the thesis

This thesis was divided into two main parts: theoretical and experimental.

In first part the main task was to present a general literature review connected with wind energy and also to define aims and objectives for following research. In this part the rules and equations needed to calculate essential parameters characterizing the turbine's performance and wake were explained. . Submission of equations from that part was needed to show how many variables and parameters have the influence on the final results and also how complicated that task was.

Second part was also divided. First part focused on description of the experiment setup and also on instruments used during the experiments. Last part, the most important one, shows results assembled during few months of the experiments. Gained outcome was analyzed, commented and displayed in charts and tables. Conclusions regarding the examined data with the most interesting parameters were drawn. In spite of the wide range of investigated cases during the project, few unanswered questions still can be found. Thus, in the end of the thesis future work tasks were proposed.

3 Overview of wind turbines aerodynamics

This chapter of the thesis is dedicated to explain fundamental rules connected with aerodynamics of wind turbines.

3.1 Energy of the wind

Every movement of the fluid is connected with energy transport. Energy carried by the wind has a lot of forms, not only potential, kinetic or thermal etc., but to analyze wind turbines with regards the power production, only the kinetic energy transfer is significant. [13]

Transfer of the energy can occur in two ways. One, when the energy is given to the wind for instance by fan or propellers that convert electric energy to kinetic energy of the wind. The second way, when the energy is taken from the wind which is elemental phenomenon of renewable energy production.

The equation that describes the energy carried by the moving air in atmospheric flow is shown below:

$$P_0 = \frac{1}{2} \cdot \rho \cdot A \cdot U_1^3 \text{ [W]} \qquad (1)$$

The energy calculated from that equation depends a lot on the velocity of the wind and the rest of variables have small influence on the final result. Unfortunately amount of energy calculated in that way is impossible to convert fully into kinetic energy. Reason of that will be explained in next chapters.

3.2 Betz momentum theory

One of the first, ideal turbine rotor models describing the power production, thrust and effect on the local wind field is called actuator disc model. It was elaborated by Rankine and Froude over 100 years ago on the example of ship propellers, Albert Betz applied this principle to the windmills in 1926 [14].

This model uses several assumptions [15]:

- Homogenous, incompressible fluid flow is characterized by steady state flow
- The rotor is represented by an infinite number of blades
- Wake is treated as non-rotating
- Pressure far downstream from the disc recovers to inlet value
- Uniform thrust over the rotor area is assumed
- No friction area is present

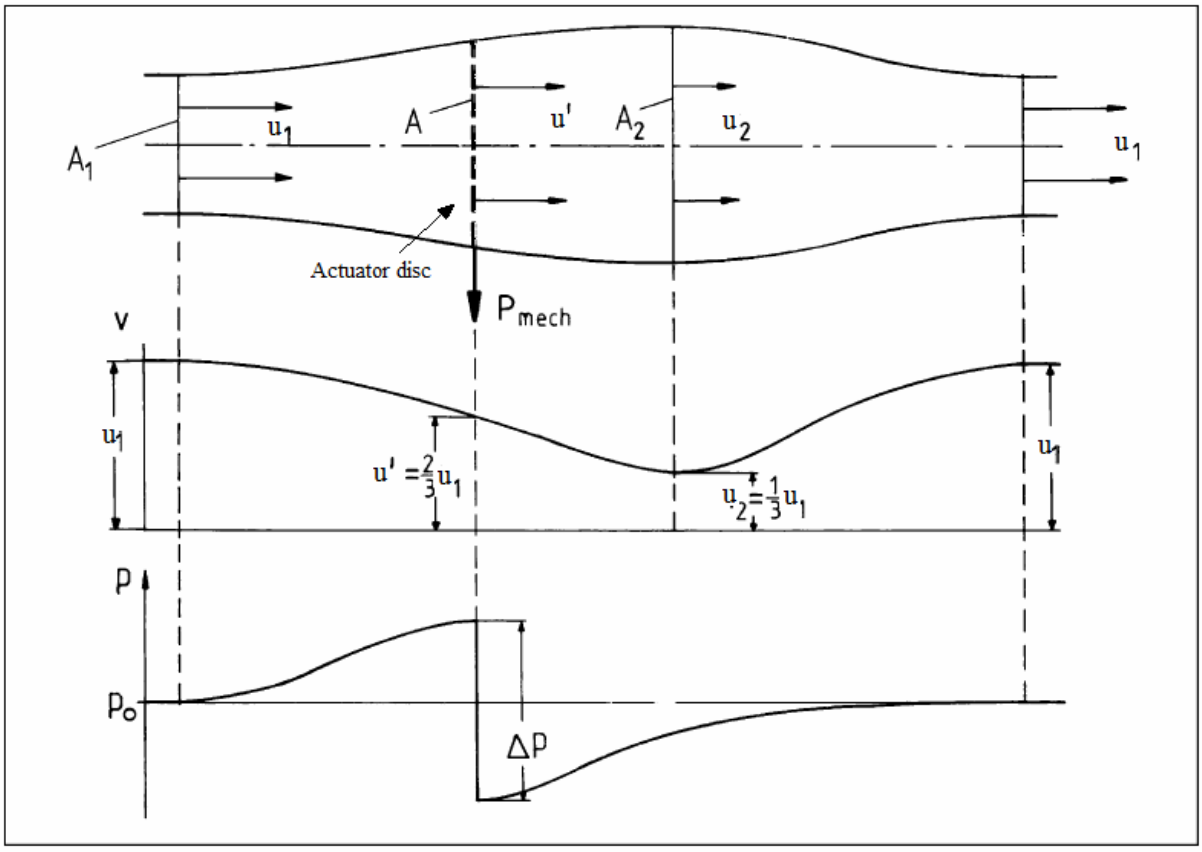

Fig. 2. Actuator disc model – velocity and pressure drop [14].

Momentum theory analysis is made for control volume of air represented by a tube with growing cross section and a rotor of the turbine represented by uniform actuator disc. (Fig. X). Free-stream airflow pass imaginary area A_1 and it is characterized by velocity U_1. At the rotor area A, energy carried by the wind is converted into mechanical energy. In the downstream of the actuator disc the maximum diameter A_2, is reached and it is corresponding

to the lowest velocity U_2. Variable diameter of the tube is caused by changes in wind velocity, which is reduced by the rotor, meaning that the tube cross section behind the actuator disc will become wider. Changes in the wind velocity are also correspondent to the static pressure fluctuations of the air. Atmospheric pressure P_0, starts to increase at a certain distance in front of the rotor plane due to blockage effect and it starts to recover again to atmospheric level downstream the rotor according to decrease of velocity. Therefore the pressure difference ΔP, can be found on the actuator plane, which can be converted to mechanical energy.

3.3 Power and thrust coefficients

After analyzing assumptions of momentum theory, the power production P of ideal wind turbine as the actuator disc can be described as:

$$P = \frac{1}{2} \cdot \rho \cdot A \cdot U^3 \cdot 4 \cdot a(1-a)^2 \text{ [W]} \tag{2}$$

,where a is defined as a ratio between the velocity deficit at the disc and the free stream velocity:

$$a = \frac{U_1 - U_2}{U_1} \tag{3}$$

Therefore, the performance of wind turbine rotor can be characterized by a power coefficient Cp, which is the ratio between power generated on the rotor shaft P and the total power included in the wind flow P_0 , usually presented as:

$$Cp = \frac{P}{P_0} = \frac{P}{\frac{1}{2} \cdot \rho \cdot A \cdot U_1^3} \tag{4}$$

or as the function of velocity ratio:

$$Cp = \frac{P}{P_0} = 4 \cdot a(1-a)^2 \tag{5}$$

Additional important parameter used to define the turbine performance is thrust T, which is equal to pressure drop on the rotor compared to its area:

$$T = \frac{1}{2} \cdot \rho \cdot A \cdot U^2 \cdot 4 \cdot a(1-a) \tag{6}$$

Similar to the power coefficient, the trust on a wind turbine can be characterized by a non-dimensional thrust coefficient *Ct,* referred as a quotient of the thrust, *T* and total power included in the wind flow P_0:

$$Ct = \frac{T}{\frac{1}{2} \cdot \rho \cdot A \cdot U_1^2} \tag{7}$$

or as a function of velocity ratio:

$$Ct = 4 \cdot a(1-a) \tag{8}$$

3.4 Betz limit

Unfortunately, as it was mentioned before, a wind turbine cannot convert all of the kinetic energy carried by wind into torque on the rotor shaft. The limitation is called “Betz limit” or “Betz law” and it is the maximum theoretically possible rotor power coefficient that ideal wind turbine can generate.

Maximum of power coefficient can be found by taking the derivative of the power coefficient form equation (5) with respect to *a* and setting it equal to zero. The result of this operation is velocity factor of $1/3$, which means maximal value of power coefficient becomes:

$$Cp = \frac{16}{27} \approx 0.593 \tag{9}$$

What is more, a maximal velocity factor means that the velocity U_2 in the wake of rotor is one third of upstream velocity U_1.

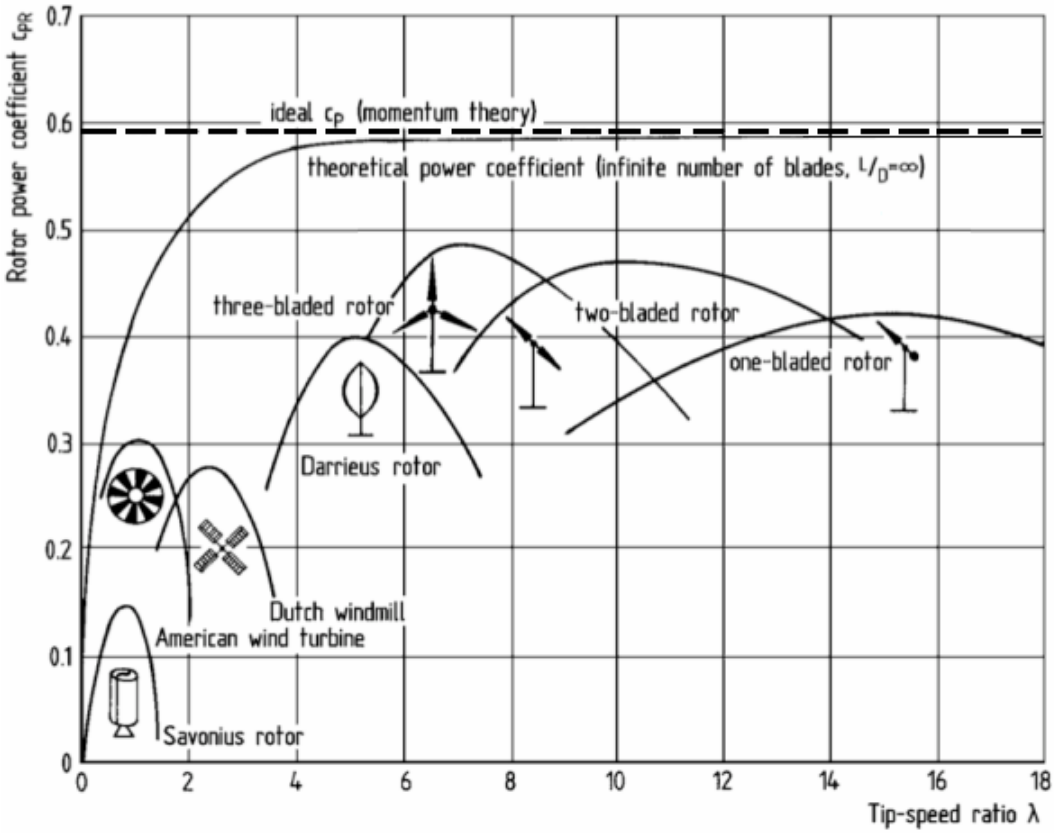

Fig. 3. Example of Cp curve for various types of wind turbines [14].

Real wind turbines will have much lower power coefficient than the ideal from Betz limit (Fig.3). There are few reasons of that phenomena: finite numbers of blades in real turbines, rotation of the wake, non-zero drag of the turbine and additional friction in the bearings of the shaft among the most important.

3.5 Tip-speed ratio

What is more, power coefficient depends on the phenomenon of rotor wake spin or even on the ratio between the rotational and translational energy components of the air stream. This ratio can be referred as a tip-speed ratio, TSR or λ, which is a quotient of tangential velocity of the rotor tip to overall wind speed.

$$TSR = \frac{\omega \cdot R}{U} \tag{10}$$

Tangential velocity of the rotor tip can be calculated from angular velocity ω and radius of the turbine R.

It is important that tip-speed ratio should be set at an optimal value to produce energy from wind turbine in the most efficient way. If the rotor is to slow to much amount of air passes

trough and energy is not fully extracted. On the other hand, if TSR is to high, big losses will appear because of high drag force on the blades. [16]

3.6 Force distribution on the blade

The wind flowing around the airfoil generates pressure difference between the lower and the upper part of the blade. Fig. 4 shows force distribution at the rotor blade cross-section. There could be found two main forces: lift and drag. The lift force is a result of the unequal pressure on the upper and the lower airfoil surfaces and it is perpendicular to the oncoming flow. The drag force is due both to viscous friction forces at the surface of the airfoil and to unequal pressure on the airfoil surfaces facing toward and away from the oncoming flow. This force is parallel to the flow [15].

Visible in Fig. 4 angle of attack α is an aerodynamic parameter parallel to real air velocity and angle between chord line and direction of rotation is called pitch angle.

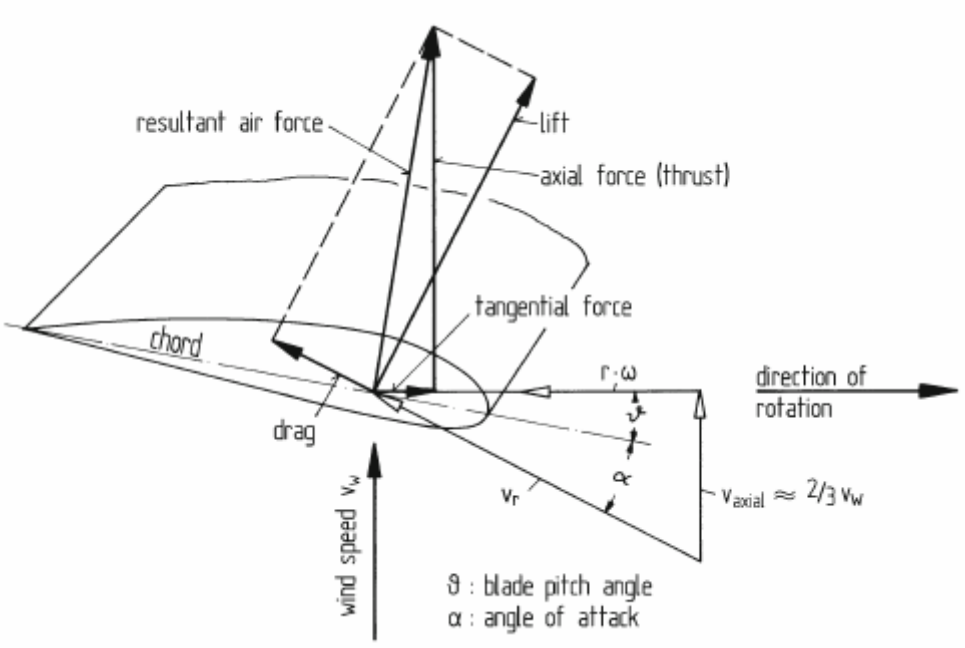

Fig. 4. Cross-section of a rotor blade with force distribution [14].

3.7 Wake and turbulence

Since the beginning of modern wind turbines development in the late 1970s wakes have become one of the main topics of research. Fully understanding of that process is still difficult and some mechanisms had not been examined yet. The reason of complicity is explained by

the fact that the inflow is always subject to stochastic wind field and for turbines that pitch angle is not regulated, stall is inseparable part of operational envelope [10]. What is more, usually rotors are made with 3 blades which also have influence on wake.

3.7.1 Rotation and vortex system in the wake

In the wake field the rotational effects and additional vortex system can be observed. The rotation of the wake is caused by turbine blades, which convert wind energy into rotational energy. Air passing over the blade exerts the torque on it what cause that torque influences on the flow. Reaction of that is creating rotational effect of the wake in countercurrent direction to the rotor [15].

Tip vortex is generated at the tip of the blade because of the difference in pressure between lower and upper surface of the blade. Size of the tip vortex is not steady, at the beginning its diameter shrinks and then it increases due to viscous effect [82]. What is more, additional vortex is formatted in the area near the rotor hub. Tip and root vortices are shown on a Fig. 5.

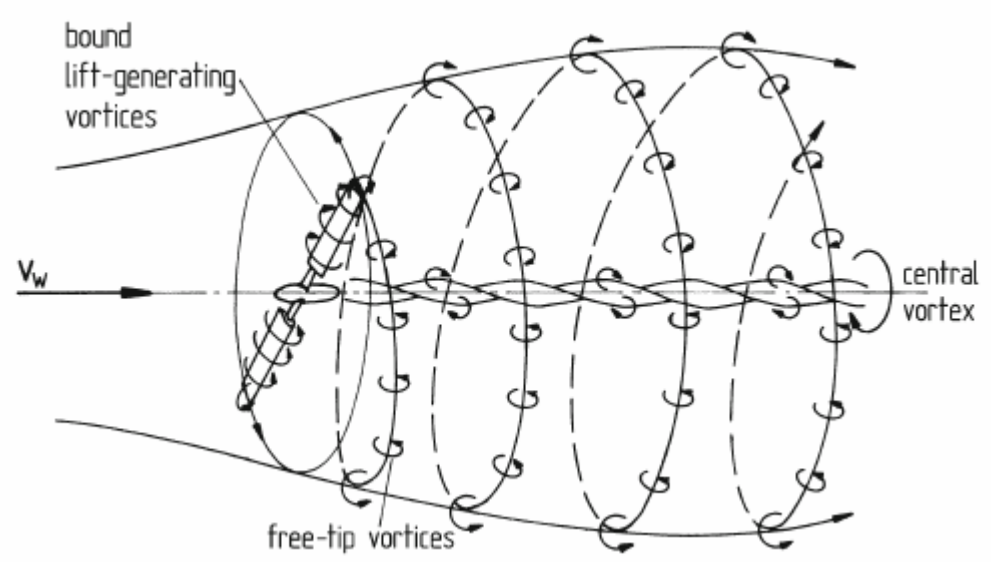

Fig. 5. Vortex model of the rotor flow [14].

Tip vortices follow helical path in downstream flow with rotation countercurrent to the rotor. When TSR or number of blades is increased distance between each vortex becomes smaller and could be even parallel to the turbine plane. Therefore, the vortex system can be described as a tubular vortex sheet. This phenomenon is also characterized by high velocity and low pressure inside the eddies.

Similar performance is also noticed near the shaft area where blades are mounted. The origins of creation of such central vortex are similar like in free-tip vortices but aerodynamic losses are much lower near the root.

The wake is divided into two main types: near and far wake area (Fig. 6). The border between them depends on the turbines parameters: size of the rotor, type of the airfoils or operating TSR and also shape of the inlet flow field. Usually the end of first type of wake ends after 1 – 2 rotor diameters downstream. Therefore, impact of the rotor aerodynamics is of primary importance, also number and type of the blades or the influence of tip vortices is significant. However, far wake is not dependent only on the rotor shape but rather on wake interference, turbulence and topographic effects what is important in designing wind farms [12].

Depending on the parameters of turbine and income flow, higher differences in pressure and velocity are noticed between outside and inside part of the wake. The tip vortices after a certain distance start to brake and create a shear layer between parts of wake. Moreover, created turbulence in the flow improves mixing between outside and inside parts . The high velocity flow region diffuses into, or mix with low velocity flow, what cause an expansion of the wake and reduction of velocity deficit. As a consequence, two peaks of the turbulence intensity are observed in the near wake, which are no longer noticeable in the far wake area. The described above a phenomenon of wake development is presented on Fig. 6.

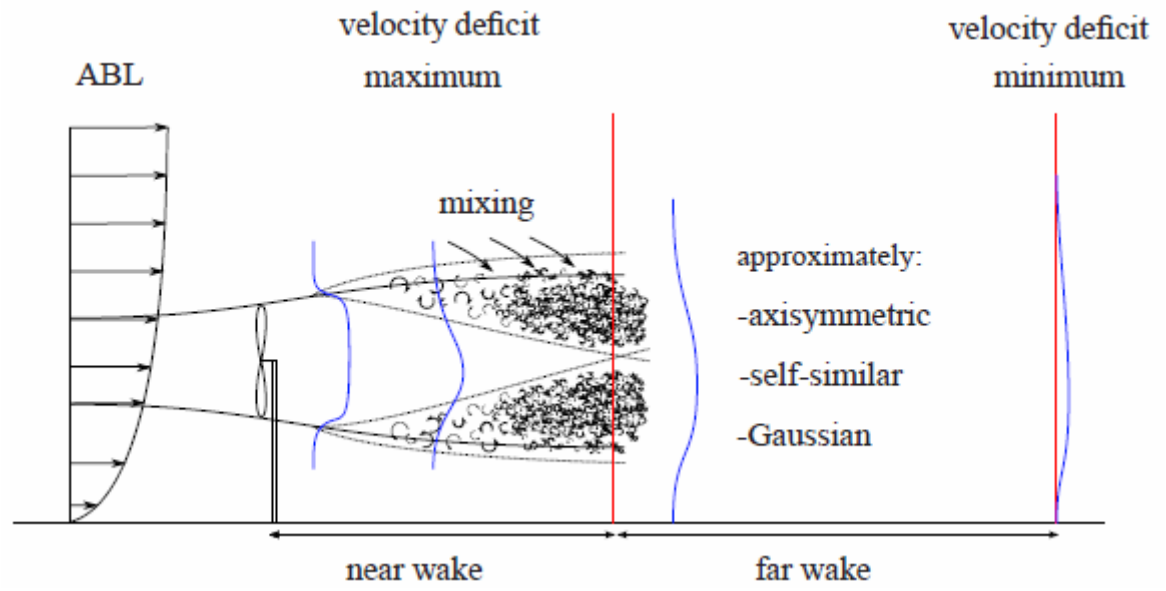

Fig. 6. Velocity and turbulence expansion in the near and far wake of the wind turbine [12].

The growth of the turbulent wake depends on [17]:

- turbulence levels in the atmosphere,

- surface constraint effects,
- wind shear effects (vertical wind gradient),
- topographic and structural effects.

3.7.2 Turbulence intensity

The influence on the wind turbine is not only determined by mean velocity. Analyzing power and torque generation of the turbine, also detailed upstream and downstream parameters are required. Therefore, one of the most important parameter being used for wake analysis is turbulence intensity, TI.

Turbulence intensity shows what are the fluctuations of the wind velocity in certain amount of time at each position. The fluctuating velocity, $U_i(t)$ consists of two parts: one, is the instantaneous velocity consisting of mean velocity, $\bar{U}$ and other one, a time dependent fluctuating velocity, $u_i'(t)$. Which is expressed by [18]:

$$U_i(t) = \bar{U} + u_i'(t) \tag{11}$$

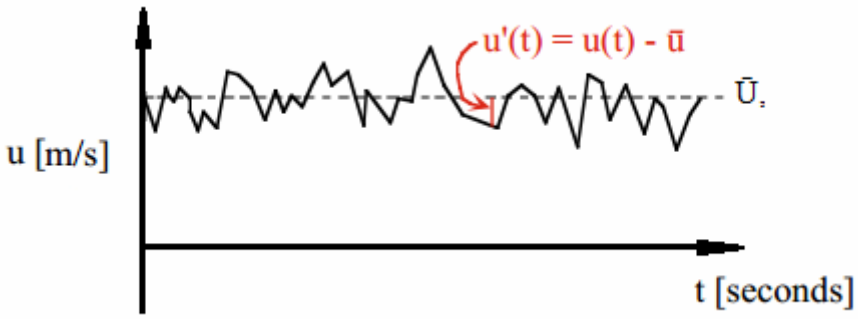

Fig. 7. Velocity recoded in a turbulent flow.

Turbulent motions associated with the eddies are approximately random, as it is shown on Fig. 7. That is why, statistical concepts are used to calculate and to determinate turbulence in the flow. The turbulence strength, u' is defined as a standard deviation from the mean velocity. The standard deviation for whole acquired sampling time instead of one certain measuring point can be calculated as follows:

$$u' = \sqrt{\frac{1}{N}\sum_{i=1}^{N}\left(u_i'\right)^2} \tag{12}$$

Therefore, turbulence intensity is described as the ratio of the standard deviation of the set of "random" velocity fluctuations, u_i' and the mean velocity, $\bar{U}$.

$$TI = \frac{u'}{\bar{U}} \tag{13}$$

Turbulence intensity sometimes has to be estimated. For that reason compared to measurements there were established a following estimations of the incoming turbulence intensity [19]:

- High-turbulence case, turbulence intensity between 5% to 20% – it could be found in high speed flow inside or behind complex geometries like heat exchangers and rotating machinery.
- Medium-turbulence case, turbulence intensity is between 1% and 5%. – it could be found in low speed flow or flow characterized by low Reynolds number like pipe flow or ventilation systems.
- Low-turbulence case, TI below 1% – it could be found in external flow across cars, submarines, aircrafts also in very high quality wind tunnels.

3.8 Wind farms

Development and steady increase of energy production from wind sources led to creation of not only single wind turbines but whole complex arrays of wind turbines called wind farms. In such wind farms the turbines are located close to each other to reduce investment costs like expenditures for area possession but also shorter electric grid. On the other hand, lower installation costs mean closer distance between turbines what causes loses in the power production. Each turbine upstream generates additional turbulence and reduce wind velocity where downstream turbines operates. Moreover, the high turbulent flow has influence on lifecycle of the rotors degrading it [20].

Fig. 8. Wake turbulence behind wind turbines – photo of Horns Rev offshore wind farm in Denmark [21].

Fig. 8 presents one of the most popular picture of wind farm near Denmark shore, where the wake effect was observed due to the humidity condensation in turbulent flow behind the rotors.

Interesting phenomenon observed during power production in wind parks is power loss of each turbine in the row. The first turbine in a row produces the highest amount of energy. In the second row high decrease in power production is observed. Thus, in next rows of wind turbines similar behavior could be expected, but generated electric energy reach similar level as second turbine in a row with slight decrease on each line. Presented behavior is presented on Fig. 9, showing results from two different wind farms (Nystad and Horns Rev).

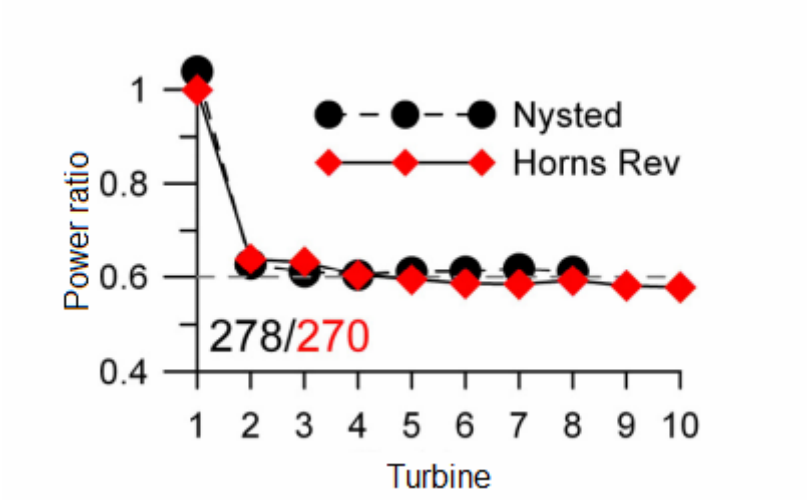

Fig. 9. Comparison of normalized power at Horns Rev and Nysted wind farms as a function of turbines position in the row [22].

Explanation of that phenomenon is found in the velocity profile and turbulence intensity evolution downstream the rotor [12]. The first turbine works in the unobstructed, low intensity homogeneous flow, where velocity is the highest from all rows. The second turbine experiences obstructed by the first turbine flow with higher turbulence intensity and lower velocity profile - the difference is even noticeable on Fig. 8. Higher turbulence behind turbine causes faster velocity recovery ,but farther down in subsequent rows of the turbines the turbulence intensity and velocity has tendency to reach some saturated level.

Nowadays, increase of wind farm energy production efficiency is one of the most important topics in wind energy sector [23]. There are numerous publications showing that that increase of the distance between turbines has significant influence on total power production due to decreasing impact of the wake effects along the distance. Wake interactions were still noticeable even at distance of 20 diameters downstream behind single turbine [24] but arrangement like that is not economically feasible due to drastic increase of area occupied by the wind farm. Other researches show that even different turbines arrangement, differently aligned or staggered arrangements has an influence on the total power production. 10% higher efficiency was noticed with staggered turbine alignment compared to in-line case [25]. Power production increased in such conditions because of the rotor of each turbine was only partly in the upstream turbine wake. What is more, the next step could be to test different distribution of the energy extraction which is carried by the wind. In classical arrangement the first row of turbines operates in best efficiency and the idea is to reduce the usage of the inlet flow and let the second row to operate in higher velocity. There are a few possibilities available to modify, for instance pitch angle of the blades and tip-speed ratio or operating an yaw angle of whole

turbine different than perpendicular to incoming wind. One already proven example is 12% higher output in power generation of the two in-line turbines where the first one is yawed of 30^{o} [26]. Moreover, small difference in TSR of first turbine from its optimal also will provide slight increase in total power production in tandem of the two wind turbines [27].

Optimization of parameters of the wind turbines operating in wind parks is still difficult task for modelers. *"Existing algorithms include only genetic algorithms and simulated annealing. There is therefore potential for improvement by using other optimization techniques, such as mixed-integer programming, dynamic programming, stochastic programming, etc…"*[23]. What is also important, numerous literature sources connected with wind farm modeling and wake development had not been analyzed in comparison with experiments. It shows that the experimental data from wind tunnel based investigation are needed for development and evaluation of calculation algorithms that are still required to be updated.

Interesting conclusion had been deducted after analyzing previous tests called "Blind Test" provided by EPT at NTNU. The idea of this set of experiments was to check accuracy of computer simulation with experimental data. Word "blind" in the name of the project means that modelers had available whole description and whole data of each test but accept the final results which should be calculated. The aim of this test series was improvement models which are used to design wind parks. Final result showed that still experimental results mismatch results from computational fluid dynamics [28,29,30].

4 Laboratory equipment review

4.1 Test rig

Equipment used in upcoming tests was used and provided by NTNU at numerous experiments as it is a typical instrumentation for wind tunnel aerodynamics studies. Similar description of apparatus can be found in many of publications and theses guided at this University.

4.1.1 Wind tunnel

Following experiments were performed in closed-loop wind tunnel shown on Fig.10 at Department Energy and Process Engineering of The Norwegian University of Science and Technology in Trondheim .

The test section of wind tunnel is 12 m long, 2.7 m wide and 1.9 m high, which is the biggest test section for academic use in Norway. The roof of the test section is adjusted for zero streamwise pressure gradient. Main fan of 220 kW total power delivers air at velocity up to 30 m/s in unobstructed free stream inside the test section.

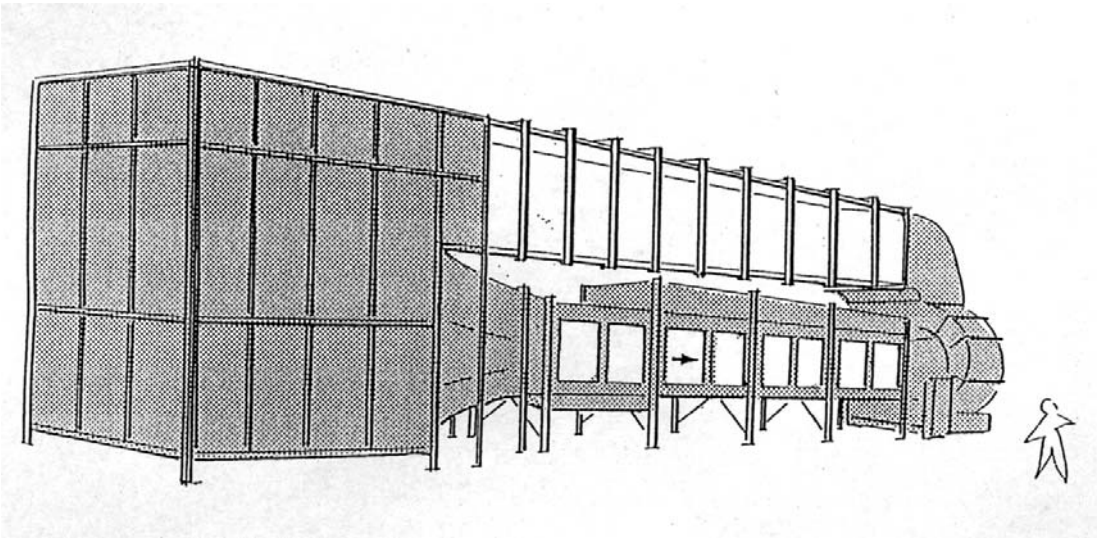

Fig. 10. The Closed Return Wind tunnel [31].

The test section is equipped with semi-automatic four-axis traversing system controlled by LabVIEW software. It was noticed during the experiments that in specific conditions traverse

size may have influence on the results – smaller cross section makes higher velocity flow underneath. For that reason also manual traverse was used to reduce mentioned influence.

The largest wind tunnel for academic research is in Italy at Politecnico di Milano where test section is 6 m long, 4 m wide and 3.84 m wide [32]. Comparing to Poland, the biggest academic wind tunnel is available at Cracow University of Technology which is slightly smaller than at NTNU with cross section 2.2 m wide and 1.4 m high of total length 10 m [33].

4.1.2 Wind turbines models

During investigations two types of horizontal axis wind turbines (HAWT) were used with three bladed rotors. One of the experimental setups is shown on the photography below (Fig.11).

Fig. 11. Setup example of T1 and T2 inside the wind tunnel [34].

The turbines were made by Hammerfest Størm AS as a prototype. Originally different type of blades were mounted but after the replacement rotor became represented as a model of existing turbine with scale of 1:100.

Both of the them were equipped with the same blades of 14% thick NREL S826 airfoils (Fig. 12) with 0^o pitch angle. This type of airfoil is commonly used in real wind turbines.

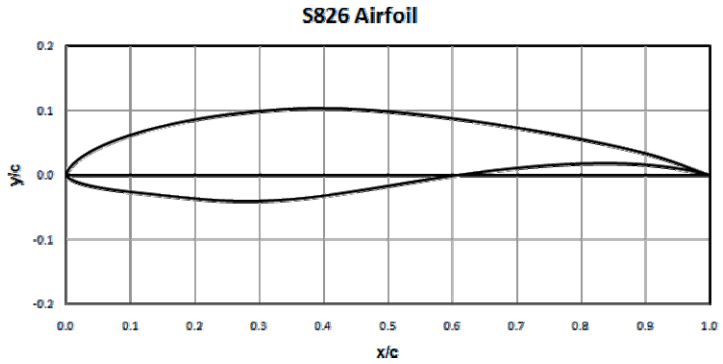

Fig. 12. Airfoil NREL S826 [35].

The turbines were designed to reach their best efficiency at a tip speed ratio TSR=6 and wind velocity 10 m/s. Because of small differences in the layout of the turbines the highest power coefficient of the first turbine called T_1 reached the peak of Cp_{max}=0.47 and for the second turbine (T_2) maximum peaked of Cp_{max}=0.45. Because of Reynolds independence area above certain velocity turbines power coefficient stays at the same level unrelated to the wind velocity fluctuations. Experiments proving stability of the power coefficient above 10 m/s for presented turbines can be found in the literature [36].

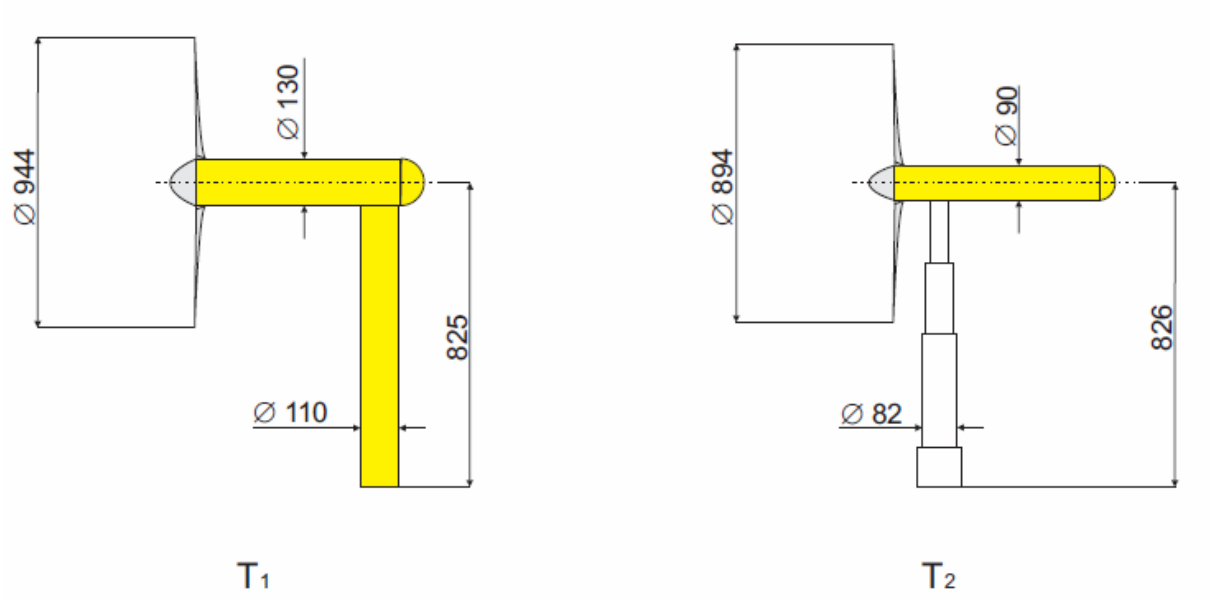

Fig. 13. Scratch with the main dimensions of the turbines T_1 and T_2.

First turbine has slightly different tower and nacelle construction than second one and the differences can be found on a scratch (Fig.13). Open construction and transmission belt outside the tower of T_2 requires to put it in the wake of T_1 where unnecessary turbulence in the wake can be reduced. Detailed differences and dimensions in the layout of the turbines are shown in appendix.

Both turbines are fully controlled by a 0.37 kW electrical asynchronous motor connected with shaft of the rotor by transmission belt. Rotation of the turbines rotors can precisely adjusted by a frequency inverters Siemens Micromaster 440. Inverter can control RPM of the rotor independently from the wind velocity, which means that in one case power is produced by the turbine and in other case it has to be delivered from the engine. Electricity gained from the energy conversion from the wind is transferred to standard electric heaters to avoid damage of the motor.

4.2 Measurement instruments

Complex investigations that were performed for the thesis need instruments that are reliable and give all variables which are important to perform the analysis of given problem. What is more important, amount of experiments requires to use an apparatus which is able to convert all responses of instruments to read them in LabVIEW software.

4.2.1 Pitot – static tube and contraction nozzle

One of the most important instrument in aerodynamics laboratory is Pitot tube. Basic function of the probe is to measure difference between total pressure and static pressure, what easily can be recalculated into velocity of the wind. In this experiments Pitot tube was used with a pressure transducer, which converts pressure to a voltage signal. The pressure transducer was calibrated with manual Lambrecht manometer.

During calibration wind velocity had been decreased from higher than usual experiment level to complete stop in 10 steps. Signal from the pressure transducer and value from the liquid manometer were written down and linear approximation was done.

The same procedure for calibration requires the pressure transducer of contraction nozzle which has holes around bigger inlet and smaller outlet to measure pressure drop. Velocity calculated from the nozzle is mean velocity at the inlet of the test section and it is used as a reference. It is important when flow inside the tunnel is not laminar and Pitot probe might be inaccurate.

4.2.2 Hot-Wire probe

The hot wire anemometry (HW) has been used for many years to measure instantaneous fluid velocity. The most important advantage of using HW is ability to measure turbulence intensity in the stream and ability to work in turbulent flow. There are also other apparatus able to work and measure mentioned conditions like laser-Doppler anemometers (LDA) and particle-imaging velocimetry (PIV) and many types of hot-wire probes which are used according to the type of fluid and it parameters.

Below investigations were executed with constant temperature anemometer (CTA) equipped with single-sensor probe (Fig.14). Size of the platinum sensor is really small: 5 μm in diameter and 3 – 5 mm in length.

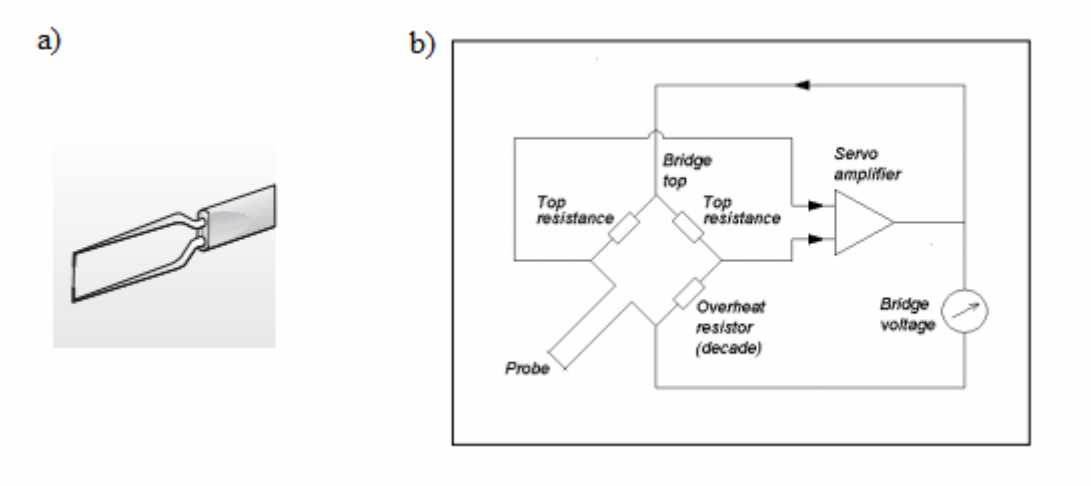

Fig. 14. Single-sensor HW probe a), Wheatstone bridge b) [37].

The main principle of operation the CTA is heat transfer from small, electrically heated wire to the surrounding flowing fluid. Constant temperature on the wire is provided by Wheatstone bridge (Fig.14), which is balanced each time when new probe is connected to it. When flow of the fluid changes near the probe, the resistance in the wire changes as well. Therefore, the fluctuation of resistance on the bridge makes fluctuation on the voltage across its diagonal. To keep the bridge balanced, the current in the wire has to increase to restore balance again – which means to keep constant temperature. Further information and deeper explanation of Wheatstone bridge and CTA can be found in references [37].

Changes in the voltage on the sensor after noise reduction and amplification are measured and stored for future analysis. Scheme of typical set of tools needed to use the hot wire (HW) probe is shown on Fig.15.

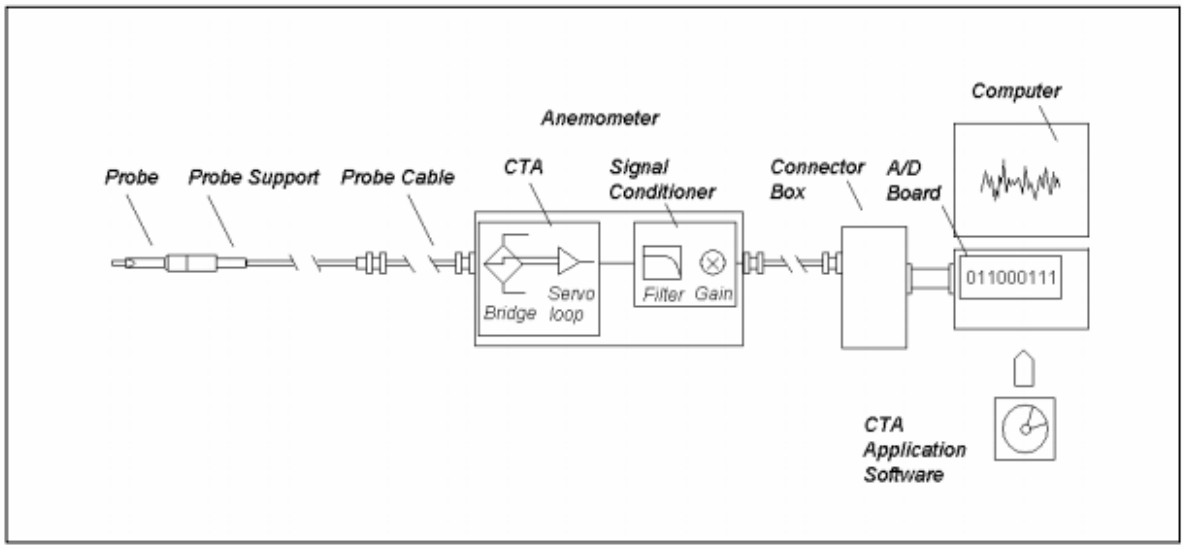

Fig. 15. Scheme of CTA measuring equipment [37].

Whole setup of HW and anemometer has to be calibrated every 1.5 hour or each time when new experiment were performed . Due to drift of the ambient pressure, anemometer, moisture etc. during the experiment calibration has been made just before and just after measurement set. Calibration is made by comparison to Pitot pressure transducer signal to HW signal. Probes were placed next to each other (approx. 50mm). 9 different velocities of the wind were used to get data to comparison. Calibration curve is non – linear whence fourth grade polynomial fit function is used to get the best alignment with error less than 1% [37]. Example of calibration curve is presented on Fig. 16.

Moreover, the important thing to mention about hot-wire probes and constant temperature anemometers is that they were built with help and guidance of NTNU EPT stuff each time when wire in the probe was broken.

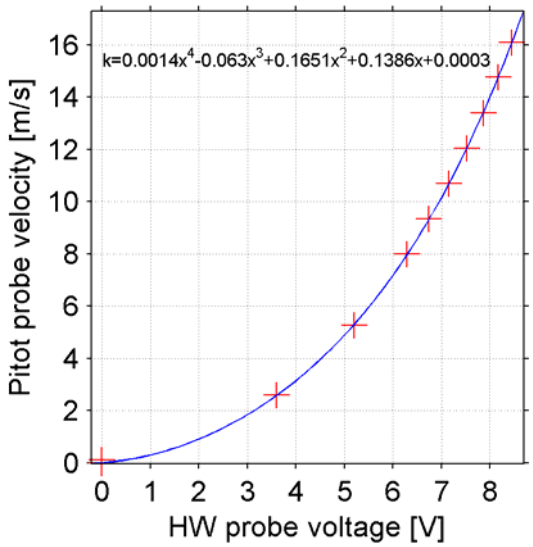

Fig. 16. Calibration curve of the HW probe signal.

4.2.3 Torque sensor

Both of the wind turbines are equipped with torque sensors T20W N/2 Nm HBM connected to the rotor shaft in the nacelle. Draft of the T_2 with mounted sensor is presented in Fig. 17.

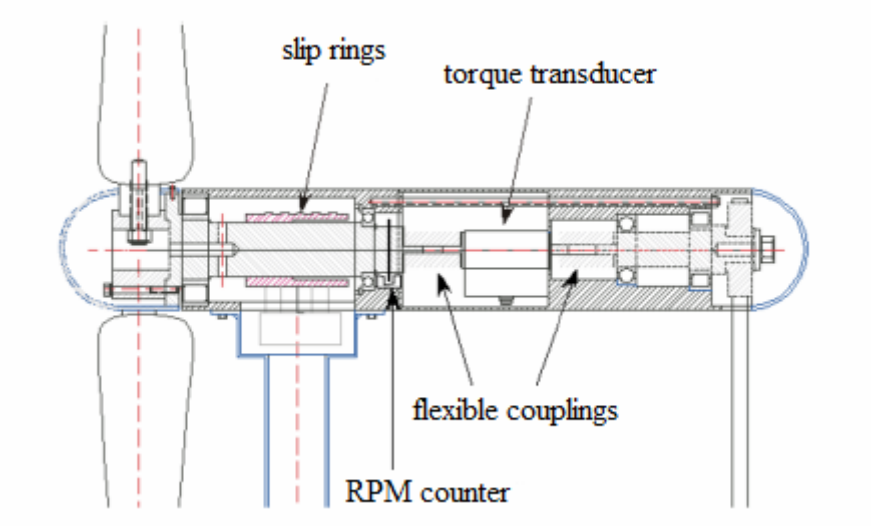

Fig. 17. Section of the nacelle of the T_2 turbine [38].

Torque transducer requires calibration. Thus, usually 5 data points with already known torque were established at the rotor shaft and each one was compared with voltage signal given from the sensor. Calibration curve is linear for T_1 and for T_2 turbine (Fig.16).

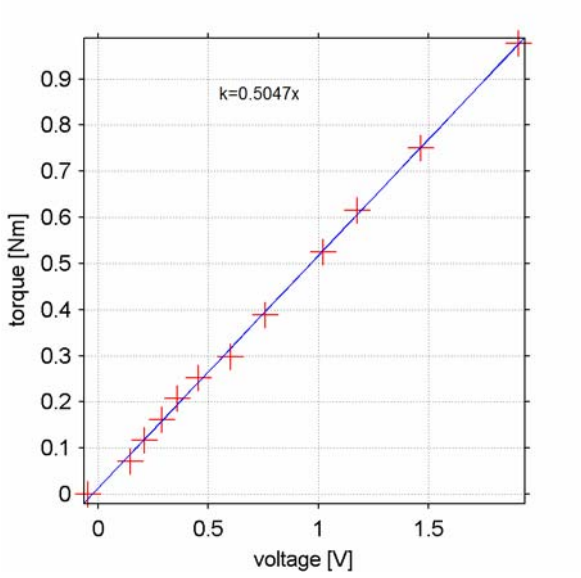

Fig. 18. Example of calibration curve of torque transducer.

Additionally, each of model wind turbines has got mounted RPM counter also shown at Fig.17.

4.2.4 Force balance and force plate

Thrust measurements were made using two types of force indicators. First turbine was mounted on AMTI 6 component force plate which is self calibrated. Second one was mounted on 6 component Shenck balance. Calibration to convert force on electric signal (V) of Schenck balance was linear.

4.2.5 Data acquisition system

Converted signals from all the transducers were delivered to data acquisition board manufactured by National Instruments (model BNC-2110). The analog signals from transducers were converted and filtered from noise in amplifiers before they reached DAQ board. LabVIEW software was used to acquire and analyze range of the signal.

Raw results when hot-wire was used were acquired with sampling frequency of 5 kHz and time 40s per one measurement point which gives 200 000 samples. It was estimated that 40s acquisition is minimal time with this parameters to fully investigate turbulence intensity in the air.

When hot-wire anemometry was not used number of samples was reduced to 100 000 with the same frequency when only Pitot probe was used to measure velocity profile along the empty tunnel. Power and thrust measurements were made with 60 000 number of samples with 2 kHz sampling frequency.

What is more important, also big attention had been put to minimize uncertainty and to increase reliability of the results. Each time, when data was acquired, the temperature was measured inside the tunnel to reduce influence of air density fluctuation. For the same reason the ambient pressure was checked before new calibration or new measurement set.

In particular cases of experiments the hot-wire anemometry technique was needed. The wire itself is really sensitive and susceptible to dust in the wind flow which may affect final results or just stop the signal acquisition. Moreover, there was observed different response of the signal for each anemometer available in the laboratory. Thus, for the most important measurements, two different hot-wire probes were used with two different anemometers at the same time to reduce risk of unpredictable failure.

However, even the best instruments can not guarantee 100% accuracy in results and every step of making experiment is concerned with errors. Uncertainties can be found in calibration, data acquisition, data reduction and also depend on type of method and others [39].

Therefore, each measurement point had long enough time series of sampling data and mean value was used in further analysis. Moreover, every file of data was characterized by root mean square, *rms* which corresponds to the deviation in each point. Confidence interval can be estimated from this value.

On the other hand, there were observed also interactions impossible to estimate which may affected the final results. For instance, one of them could be external influence on a signal from different instruments or even other signals itself. Surprisingly irregular usage of electric grid or usage of the same socket caused jumps in a signal. Similar behavior of signal changes was noticed when transducers were placed next to each other or near to AC/DC converters. Next example of immeasurable signal influence could be proper grounding of the instruments and the turbines as well as proper setup of inverters before experiments. The first acquisition point, when velocity of the wind was stopped (0 m/s) and no forces were visible on transducers was also important. This value had also significant influence on the final results.

Except the signal influence factors, there could be found more parameters that overestimated or underestimated final results. First of them is inaccuracy of the blades pitch angle setup, which might be shifted after a time or axial displacement and yaw angle of the wind turbines in next distances. Secondly, experiments where high turbulent inlet flow was required. Because of close distance from the grid to the low pressure pipes at the contraction nozzle reference velocity might be affected. Next serious problem could be an unbalanced shaft of the one turbines rotor. Surprisingly, vibrations of the shaft were transferred to the force plate and in certain RPM amplitude of oscillations was higher than the force plate range could cover.

Nevertheless, all of possibilities that might have influence on the final results had been reduced to the possibly lowest value. Some experiments, where the disorder was found, had been made again or when disorder was significant results excluded from this thesis.

5 Experimental setup

Experiments made for the thesis performed at Process and Energy Department NTNU were divided into few main steps:

1. Best power operation point for an in-line array of two wind turbine models in different distances along the tunnel. Final aim of the experiment is to find the optimal operational parameters of the wind farms and the amount of energy gained after corrections of the rotors spin.

2. Horizontal wind velocity and turbulence intensity check behind first turbine in the distance where power coefficient of second turbine was measured (referring to experiment 1). Results could be compared with full scale wind turbines and show flow profile in far wake experienced by next turbine in a row. Recovery of the velocity along the distance and its influence of the power production can be found.

3. Vertical wake development between an in-line array of two wind turbine models. Carried experiment shows difference between part of the wake behind tower of the turbine and the stream obstructed only by the rotor. Second aim was an attempt to find interaction of turbine for upcoming flow stream.

4. Repetition of previous experiments, but with turbines operating in high turbulent flow. Experiments where conditions are close to the natural (here: TI) can give an overview of disagreement with wakes created in ideal wind tunnel tests. The performance of array of the two in-line wind turbines in close to real life conditions of wind farms could be also interesting.

Big effort had been made to get precise results of the experiments. Thus, some part of experiments was devoted to evaluation of previous tests made at the wind tunnel laboratory at NTNU for making them as much reliable as possible. Nevertheless, big number of measurements has never been done before, what makes them unique for researcher scale. Outcome of the experiment will improve knowledge and provide better understanding of complex wind turbines interactions. Moreover, those results will be useful for upgrading

simulation models which are used to design new wind farms. This , in the end will boost the development of wind energy in the future.

5.1 Cp and Ct measurements

The main aim of this project was to find the best power production of the two in-line turbines. For that reason TSR of T_1 was established as constant and TSR of T_2 was changed step by step and each time torque from the rotor shaft was measured. When Cp curve of T_2 was made, the TSR of T_1 was changed again to create matrix of results. Operational parameters of both turbines are shown below. The same conditions were repeated also with the grid measurements (for different inflow turbulence intensity level).

- Tip-speed ratio of T_1: 3 – 10 with step of 0.5
- Tip-speed ratio of T_2: 1 – 9 with step of 0.5
- Distance of T_2 behind T_1 (X/D)= 3, 5, 9

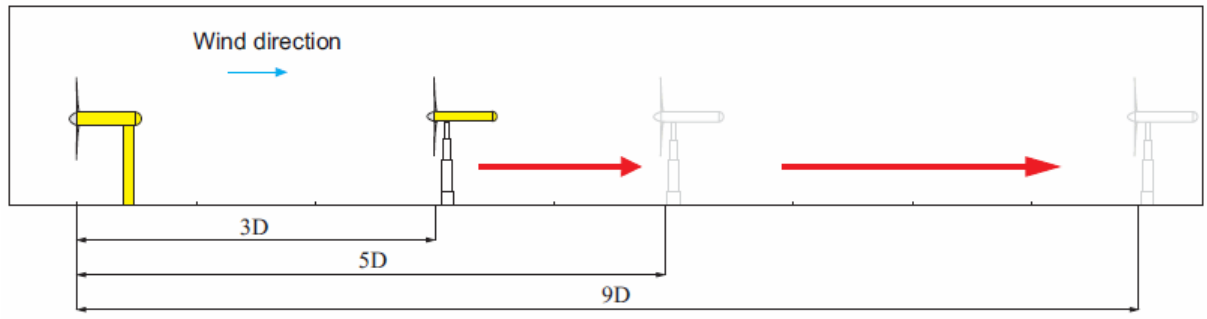

Fig. 19. Power measurement setup.

5.2 Wake measurements behind T_1 - horizontal

Second main goal of the experiment was to check what is the velocity at which the second turbine worked in previous set (in experiment 1). Wake distribution behind the turbine was measured in horizontal direction on hub height using single hot-wire probe with CTA anemometer.

Repeating all previous operational parameters of T_1 was unnecessary because of small differences in wake parameters That is why TSR of T_1 was chosen where the best power production was found.

Unfortunately automatic traverse mechanism was not able to be moved further than 8.5D behind T_1 instead of 9D.

- Tip-speed ratio of T_1: 5, 6, 7
- Distance behind T_1 (X/D)= 3, 5, 8.5

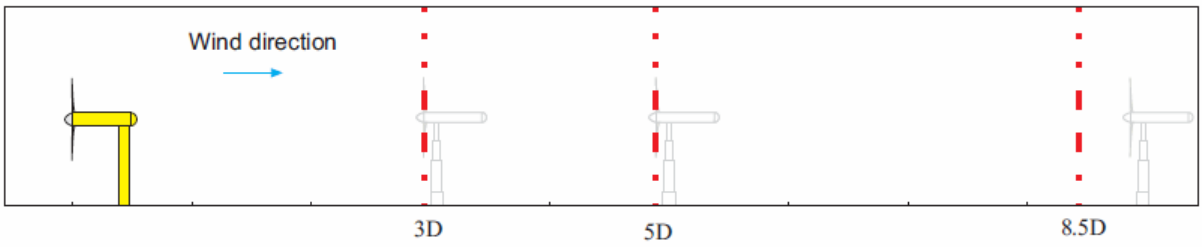

Fig. 20. Setup of the horizontal wake measurements.

5.3 Wake measurements between two model turbines - vertical

Third part of investigations was connected with behavior of the wake which can be affected by blockage of the downstream turbine. For this experiment the automatic traverse mechanism was put out from the test section. It was highly possible that the traverse could have serious influence of the results. The manual traverse cross section is much smaller than in the automatic one therefore influence of the wake would be reduced.

Disadvantage of using manual traverse is that it is inconvenient for user and what is the most important measurements can be provided only in vertical direction.

Upcoming parameters were established for this test:

- Distance of T_2 behind T_1 (X/D)= 9
- Wake measurement distance behind T_1: 3D, 5D, 8D, 9D (without T_2)
- Tip-speed ratio of T_1: 6
- Tip-speed ratio of T_2: 5, 8 (without the grid only)

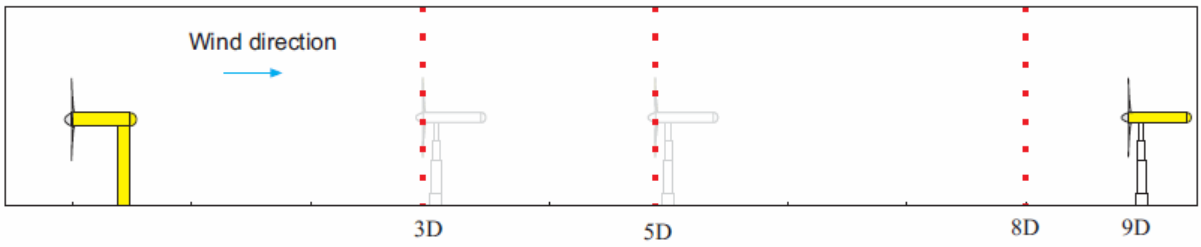

Fig. 21. Setup of the vertical wake measurements.

5.4 The Grid

Wind in real conditions is distributed with higher turbulence intensity than it is given in the laboratory conditions. That is why, to increase turbulence intensity in free stream flow in the test section the special grid had been used. The grid model was placed at the inlet of test section in the tunnel, 2D in front of T_1. It was wooden construction with biplane bars which covered whole cross-section of tunnel . The grid mesh size was M=240 mm with thickness of the bars L=75 mm.

Although, dispersion of TI and velocity of the wind in environment is not symmetrical. Turbulence intensity profile decreases with height from the ground and wind velocity increase with the rising level of height. In presented measurement set, the generated high turbulence intensity in free stream flow was undistributed on the height.

6 Results and discussion

6.1 Introduction – reference velocity, empty tunnel

Reference velocity during the experiments was measured with one the following ways. When there was no grid inside, Pitot probe was used as a reference instrument and when the grid was mounted, the contraction was used to calculate velocity. Mean velocity was established at U≈11.5 m/s. It was enough to reach Reynolds independent region for the wind blades – therefore dimensionless operation parameters are unrelated to the wind velocity.

Pitot probe was placed 500 mm from the inlet, on hub height 300 mm from the wall of the wind tunnel.

Turbulence intensity was checked before performing the experiments in intended turbines locations. Mean turbulence intensity over the area swept by the rotor is shown in table 1.

TI at:	0D	3D	5D	9D
No grid	0.20%*	0.23%*	1.00%*	1.30%
Grid	11.1%	5.01%	4.00%	3.31%

Table. 1. Turbulence intensity distribution in the empty wind tunnel.

Different TI levels were observed when the grid was mounted at the inlet of the test section than without it. Low turbulence intensity profile was rising along the distance to reach 1.30% in the last spot (9 D) – which is relatively small value. Turbulence intensity with the grid at the inlet position had the tendency to decrease along the downstream. The highest TI=11.1% was measured at the position of the first turbine and it reached the bottom at TI=3.31% at 9D distance. Results with the symbol *, for low turbulence stream flow were found and estimated from Adaramola and Krogstad measurements [36], and previous “Blind Test” [30].

6.2 Power production of two in-line model wind farm

Investigation of electric power production by a tandem of model, scaled in-line wind turbines was the main part of the project. Following results will answer questions connected with influence of the operation parameters of the first turbine on the second one, working in the wake conditions.

What is more important, experimental optimization of the power production of two wind turbines tandem has never been carried in so wide scope. Current research was done not only when distance between turbines was adjusted, but also operational parameters of each turbine and the wind were changed. Furthermore, increase of the energy output with will be of paramount importance for improving the efficiency of real scale wind farms.

6.2.1 Low turbulence intensity stream flow

- 3D distance

Power performance of the two in-line wind turbines operating at 3D distance between them is presented in Fig. 22. Surprisingly, the best efficiency of this wind farm was gained when both turbines did not work in their optimal, designed parameters, which is separately TSR of 6.0 for unobstructed flow. The peak power output was 10.7% higher if the T_1 was operating at TSR=4.5 and T_2 at TSR=4.0. Power coefficient reached their highest level of Cp_{total} =0.593 and it was gained by Cp=0.453 of the first turbine (instead of the best 0.468 in this conditions) and Cp=0.140 of second one. Nevertheless, area with high power coefficient above 0.55 is available when turbines work at TSR=4.0 – 7.0 for T_1 and for T_2 at TSR=3.0 – 5.0.

As it was expected the Cp of second turbine reached its highest value when T_1 was operating at low tip-speed ratio or much higher than optimal. Although, even when T_1 was close to runaway, the Cp of the second turbine did not reach level of low TSR of T_1.

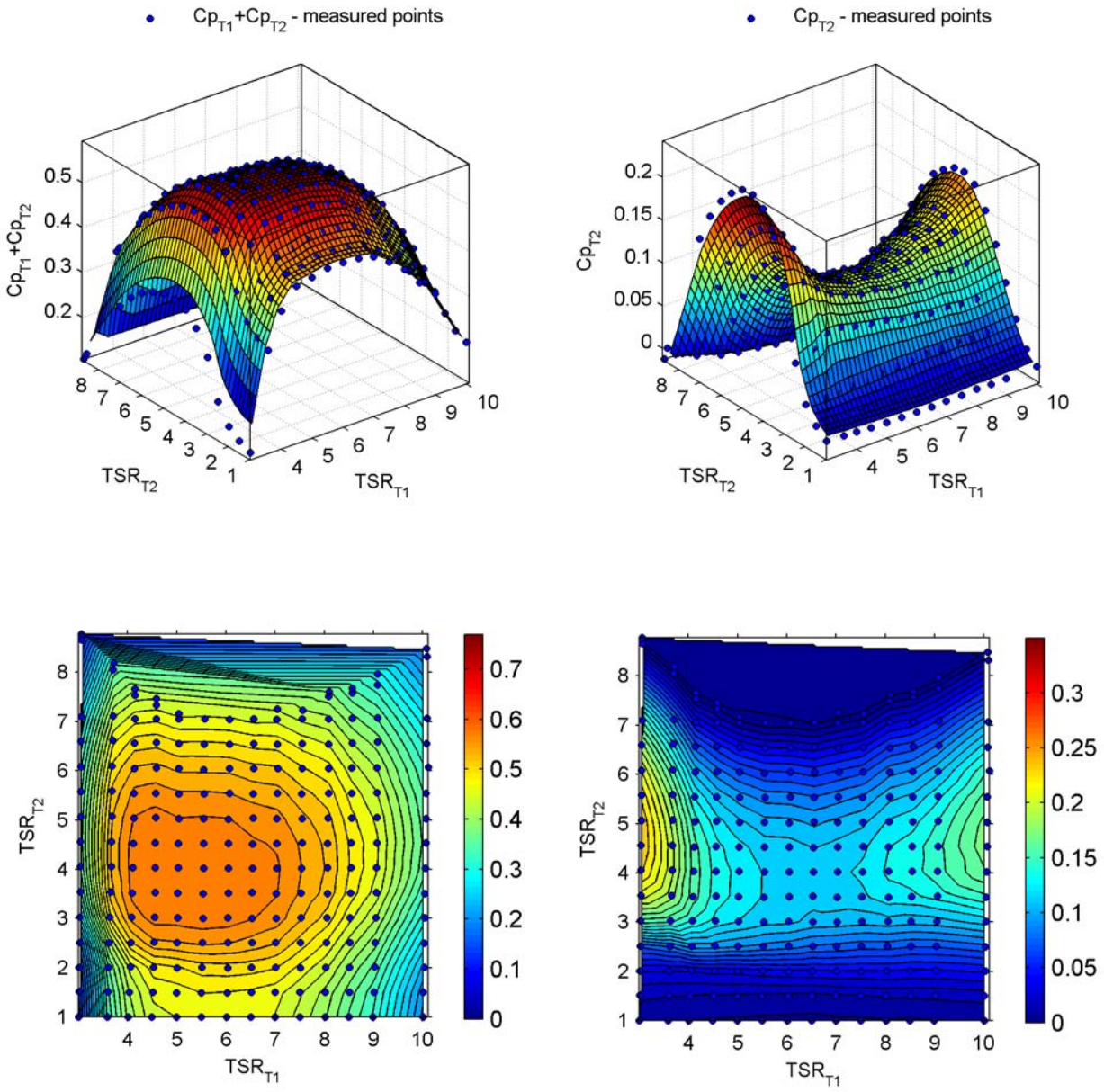

Fig. 22. Power coefficient of two in-line wind turbines – left side, power coefficient of T_2 operating in the wake of T_1 at 3D – right side.

- 5D distance

Fig. 23 shows power coefficient behavior according to framework of both turbines. Likewise it was before, results have the tendency to be shifted from theirs optimum. For this case top of efficiency reached the peak at Cp_{total} =0.628, when T_1 was operating of TSR=6.5 at Cp=0.475 and T_2 of TSR=4.0 of Cp=0.153. Total efficiency of wind farm increased 8.35% than it was measured for TSR=6.0. Range of TSR of first turbine between 4.0 – 7.0 and second turbine between 3.0 – 5.0 allowed to reach high power coefficient over 0.6. Obviously area of the highest Cp from previous test case (3D) was much wider.

Corresponding results were observed after analyzing of power coefficient from second turbine only. There were also two peaks with high Cp, when first turbine was operating in much higher or much lower TSR than optimal.

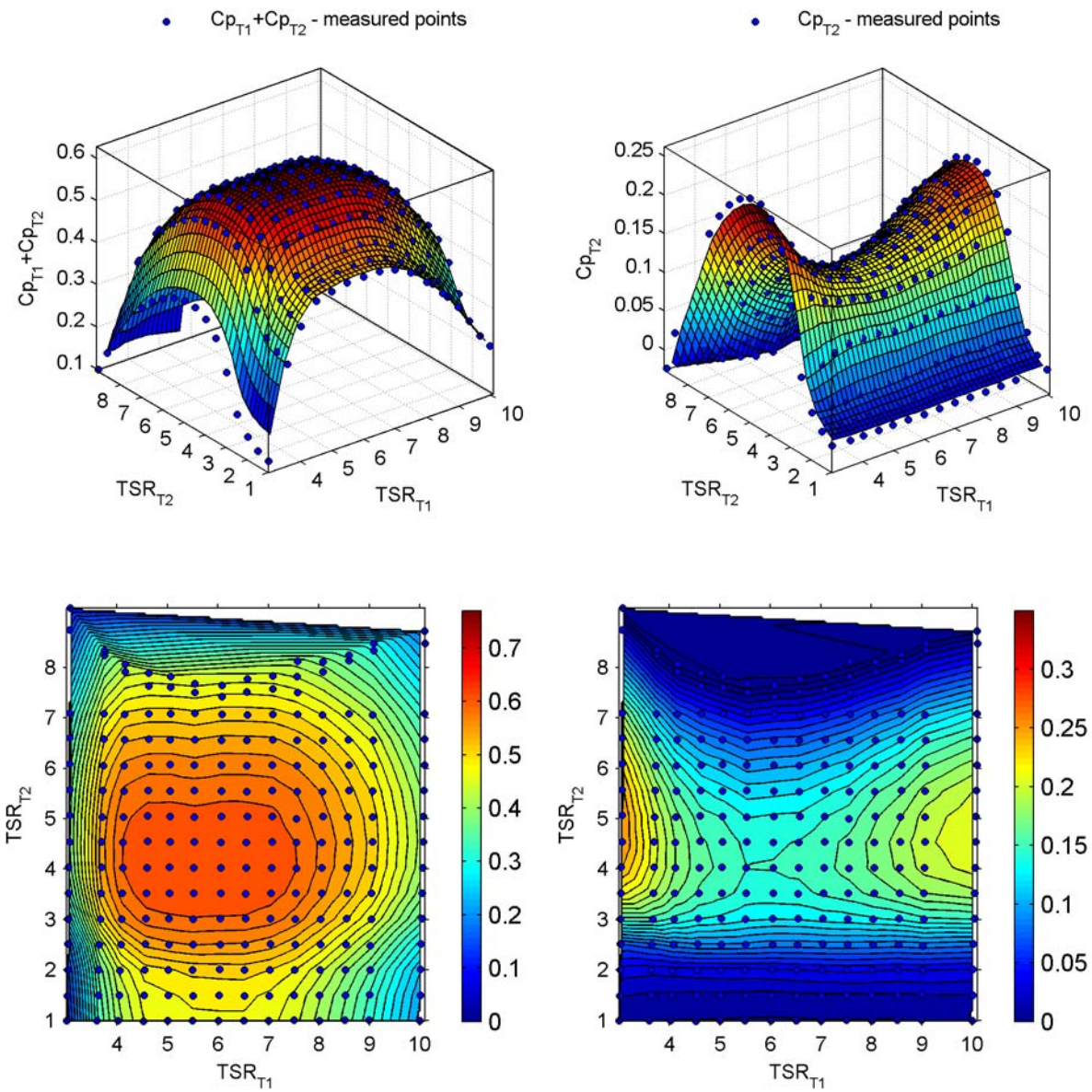

Fig. 23. Power coefficient of two in-line wind turbines – left side, power coefficient of T_2 operating in the wake of T_1 at 5D – right side.

- 9D distance

Experiment made at 9D separation distance between turbines gave also expected results of total power production of wind turbines tandem. The biggest power outcome was achieved when both of the turbines work at TSR=5 of Cp=0.470 for the first turbine and Cp=0.250 for the second one. Total power coefficient was calculated as Cp_{total} =0.720 and it was by 4.08%

higher than at designed tip-speed ratio. This time, the area of highest total Cp shown on Fig. 24 was characterized by TSR=4.5 – 7.0 of T_1 and TSR=4.0-6.0 of T_2.

Moreover, there was noticed different behavior of the second turbine performance in comparison with previous measurement (5D). Peaks with higher Cp were also detected in low and high TSR of the first turbine, but near the optimal working parameters deficit of power production was insignificant (0.1 of difference between maximal and minimal point).

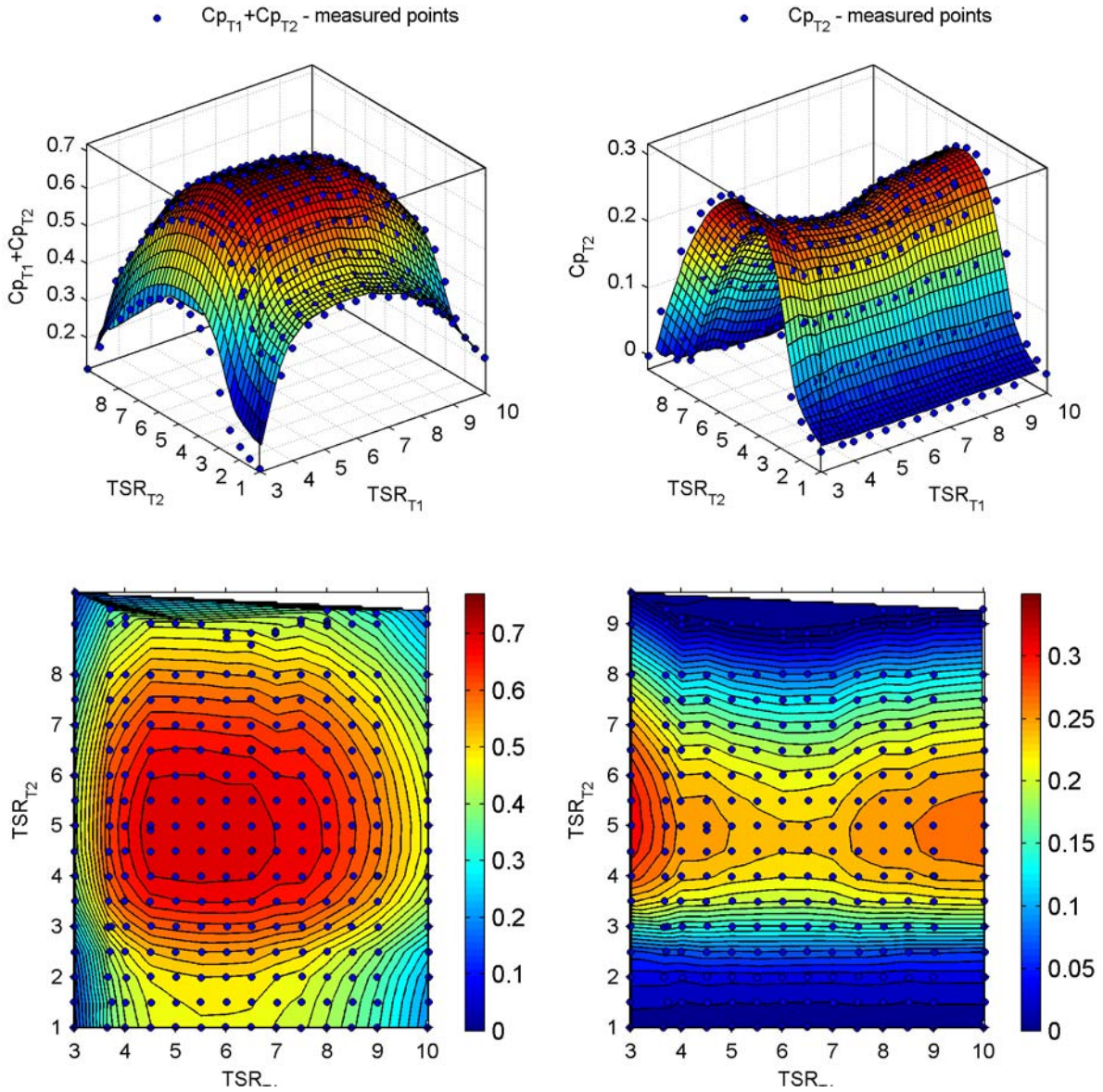

Fig. 24. Power coefficient of two in-line wind turbines – left side, power coefficient of T_2 operating in the wake of T_1 at 9D – right side.

6.2.2 High turbulence intensity stream flow

- 3D distance

Results obtained from 3D separation distance test case for the turbines operating at turbulent inlet flow are presented at Fig. 25. The most interesting part of this research is maximal power coefficient of arrayed turbines which climbed to Cp_{total} =0.623 (5.05% higher compared with same setup but for low turbulence intensity inflow). The tip-speed ratio of the best efficiency was noticed when the first turbine was working at TSR=5.5, when Cp of this turbine reached 0.474 and the second turbine was working at TSR=4.0 of Cp=0.149. Area of operational parameters when high power production (Cp above 0.60) was acquired is characterized by the first turbine TSR=4.5-7.0 and the second one TSR=3.0-5.0. The 9.49% growth of power production was observed with such adjusted TSR than for nominal operational conditions for separate turbines.

Considering only the behavior of the second turbine, the drop of power coefficient due to the best performance of the first turbine can be observed, but not as sharp as in low turbulent flow case. The difference between the highest peak of T_2 Cp and its minimal point was measured to be approximately 0.1.

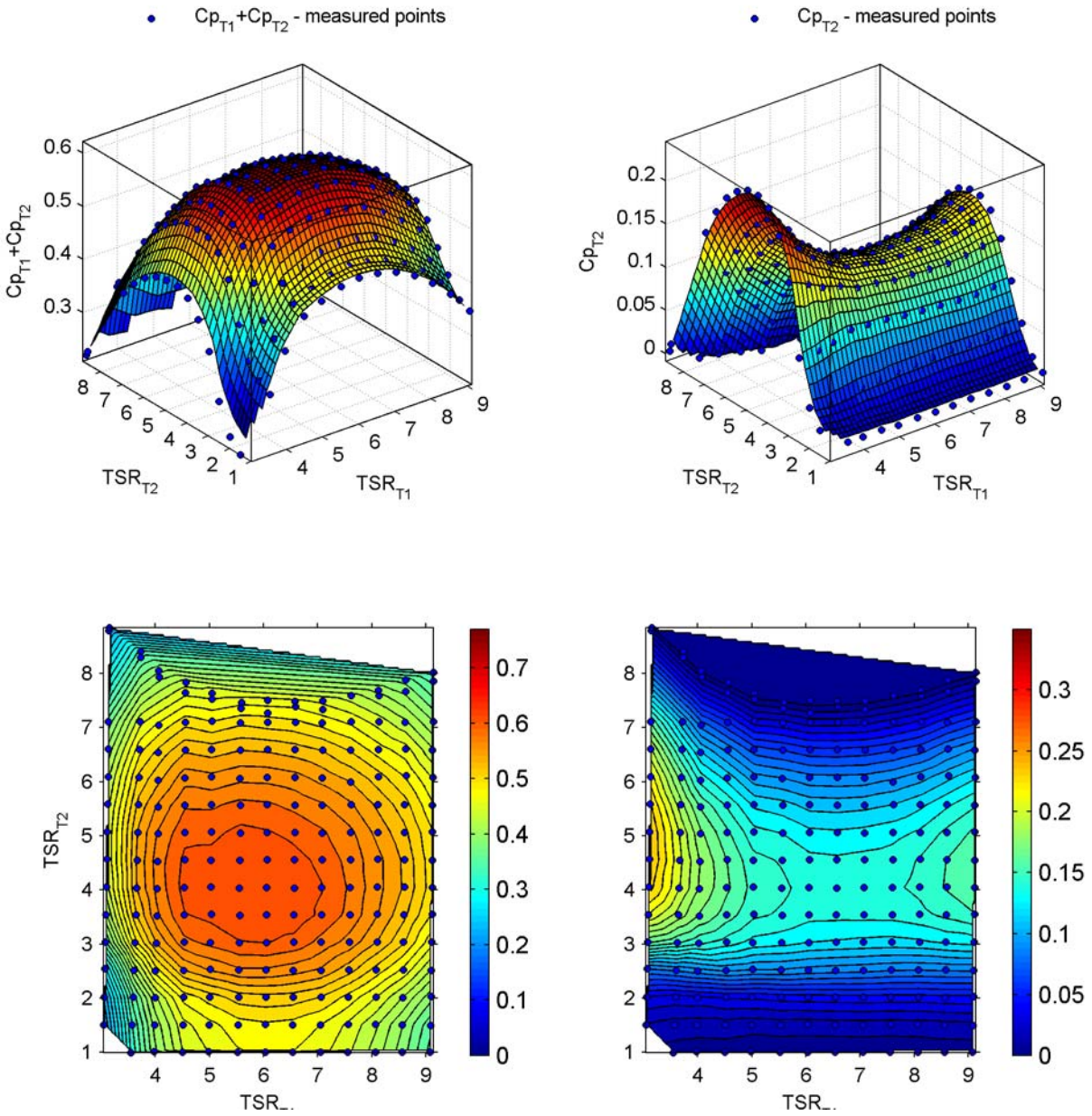

Fig. 25. Power coefficient of two in-line wind turbines – left side, power coefficient of T_2 operating in the wake of T_1 at 3D – right side.

- 5D distance

At 5D separation distance there was also noticeable increase in total power production. Maximum power coefficient reached value of Cp_{total} =0.670 when T_1 was operating at TSR=6.0 of Cp=0.480 and T_2 at TSR=4.5 of Cp=0.190. Gained power was 5.69% higher if both turbines operating at TSR=6.0. Combined Cp profile has been more steep than in closer distance case and than in the experiment at the same separation length, but without the turbulence introducing grid. Area with high power production was more narrow than it was

before (shorter separation distances) but still quite wide. Cp above 0.65 was reached at TSR=4.5-7.0 for first turbine and TSR=3.5 – 5.5 for the second one.

Power coefficient of the second turbine is presented on Fig. 26. Corresponding to the test without the grid, area of high efficiency was significantly smoother and higher. The variation between extreme values was smaller than in 9D no-grid case with the Cp difference around 0.07.

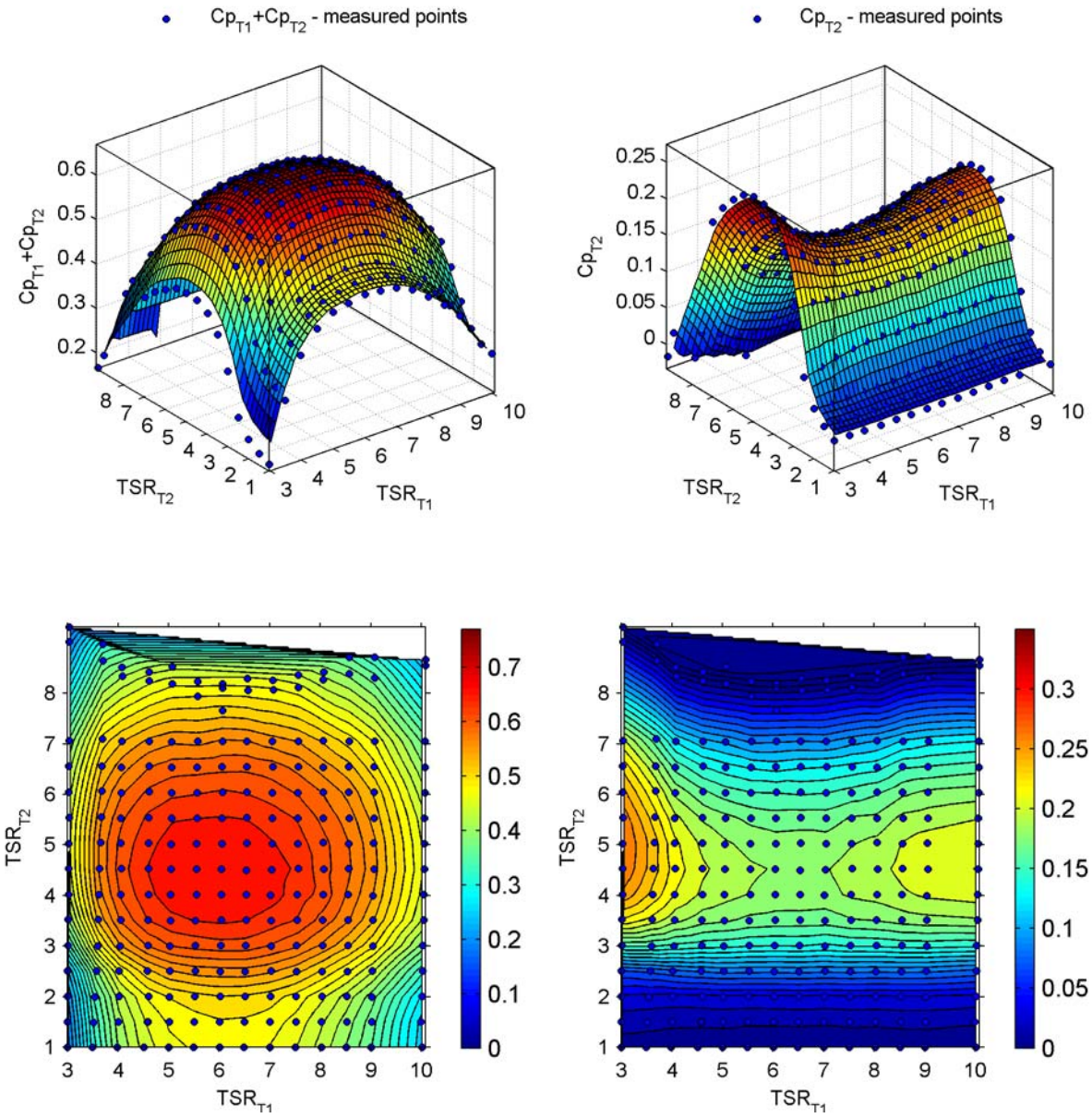

Fig. 26. Power coefficient of two in-line wind turbines – left side, power coefficient of T_2 operating in the wake of T_1 at 5D – right side.

- 9D distance

Fig. 27. presents results from 9D separation distance case electric power measurements. Total power production from two wind turbines gained Cp_{total} of 0.762 with Cp=0.481 given from T_1 and Cp=0.281 from T_2. Tip speed ratio of the first turbine was established on its optimal value of TSR=6.0 and the second turbine was performing at TSR=5.0. Changed TSR of the second turbine would cause slight reduction of power output around 2.09%. Similar to previous distance (5D) also here the area with much better efficiency is present. Power coefficient higher than 0.70 was reachable for following set up of the first turbine TSR=4.5 – 7.0 and for the second one TSR=4.0 – 6.0. The second turbine power behavior was almost independent from TSR of T_1 when its TSR (T2) was higher than 5.0, marginal fluctuation observed. Moreover, the difference between Cp, when TSR of T_1 was 3.0 and the lowest Cp when T_2 was operating at TSR=5.0 was less than 0.06.

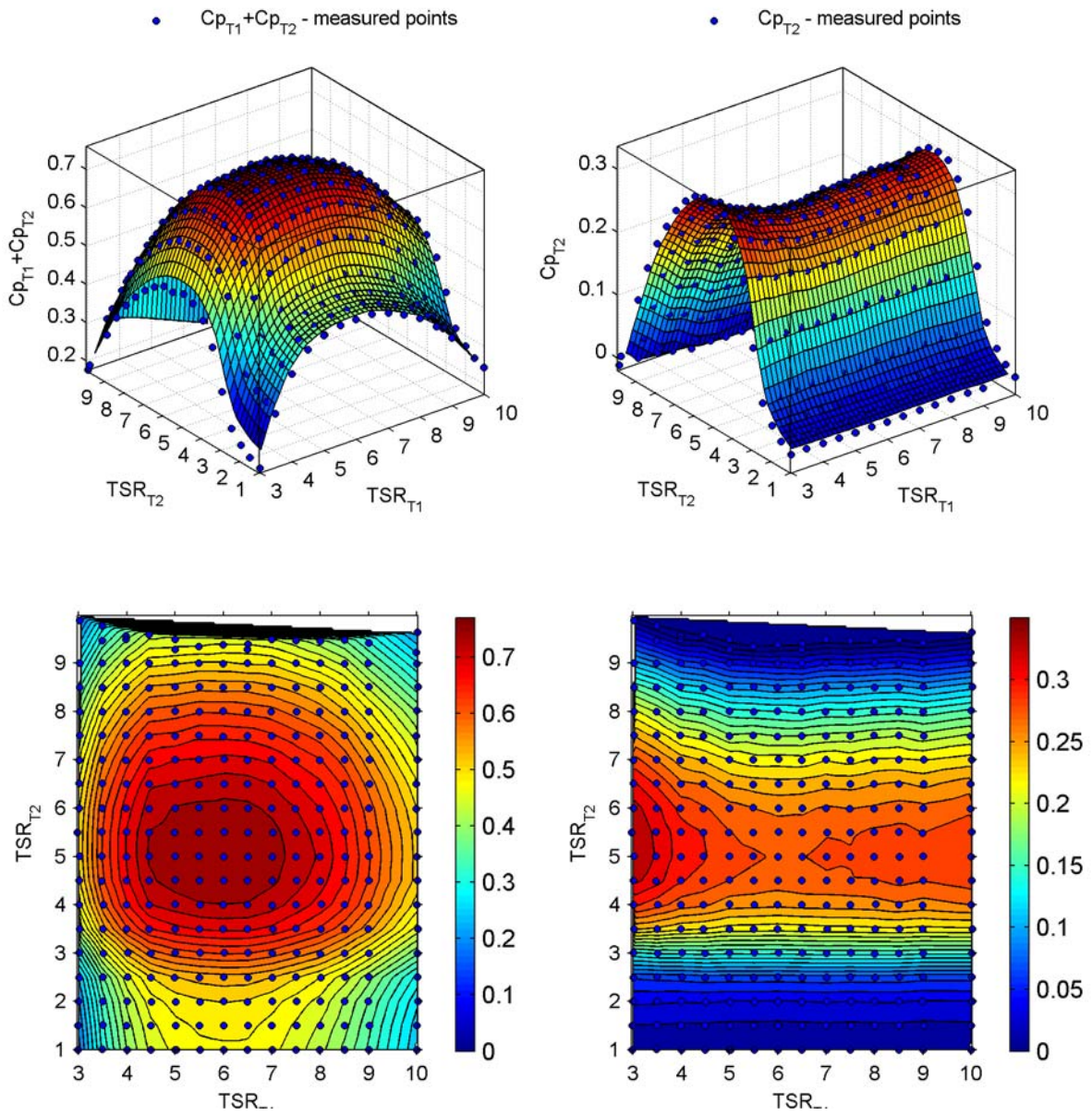

Fig. 27. Power coefficient of two in-line wind turbines – left side, power coefficient of T_2 operating in the wake of T_1 at 9D – right side.

6.2.3 Review of power production measurements

After analysis of the first part of obtained during the power coefficient investigation data few conclusions were found:

- Total power production of two turbines is increasing with increase of the distance between them. Spacing from 3D to 5D gives increase of 5.9% in power output when the turbines operate in laminar inlet stream and 7.5% when inlet flow is turbulent. Further separation from 5D to 9D cause even higher growth in total Cp gained from the wind farm by 14.6% and 13.6% in accordingly low and high turbulent stream.

- High turbulence intensity in the income flow causes visible grow in Cp of the second turbine, what also influences the total power production of both turbines. Observed growth range of total power production fluctuated from 5.0% to 6.7% for each distance setup. Also, the shape of the maximum Cp curve of the second turbine was much smoother for turbulent inflow (when the turbulence introducing grid was mounted).

- A very interesting parameter, that seems to be omitted in previous investigations, should be paid attention to is a tip-speed ratio behavior when the highest efficiency of wind farm is achieved given. For optimal Cp results with low turbulence inflow TSR of the first turbine has never been optimal, but it was oscillating from 4.0 to 6.5. In the other hand, when there was the grid inside the tunnel, the TSR of first turbine was always at 6.0. Reason of that could be found in different wake behavior for different inflow turbulence intensity with and without the grid, which will be analyzed in further chapters. Moreover, influence of adjusted TSR of the turbines had tendency to be lower along the distance and it was even less in turbulent flow.

- The second turbine, working in the wake of the first turbine has reached its maximum Cp at TSR ranged from 4.0 to 5.0, depending on the separation distance, but it was found to be independent on the first turbine TSR.

- Top Cp value for the second turbine was never higher than for the case when the first turbine was operating at the lowest tip-speed ratio, even in the runaway.

6.3 Horizontal wake development behind single wind turbine

The second aim of the project was to investigate the velocity and turbulence intensity development of the wind behind the first turbine of the wind farm. This research can illustrate exactly wind parameters which were experienced by next turbine in a row. As it was shown in previous chapter, even the slight modifications of the wind parameters had essential impact on the power production. Moreover, wake modeling of the flow is still one of the most difficult tasks for modelers. This type of simulations requires solving complex mathematical problems and what is more important it needs huge amount of computer resources. Nevertheless, existing models simulating wakes still have to be improved by comparing them with the experiments.

Wake measurements were performed before at NTNU with the same type of turbines at [26, 28, 29, 30, 36, 40, 41] but previous experiments were always connected with close region behind T_1 or they do not cover the parameters range investigated in previous chapter (power investigation).

In following experiments the automatic traverse was used and measurements were taken only in horizontal direction on hub height of the turbine. As it was mentioned before, three different TSR levels of T_1 were investigated: TSR=6 which was optimal for first experiment and also one lower than optimal (TSR=5) and one higher (TSR=7).

Results are shown on the figures below: on the left, the mean velocity profile and on the right the turbulence intensity for each distance. Additionally, to sum up the results for given distance, the description table was generated with the most significant values.

6.3.1 Low turbulence intensity stream flow

- 3D distance

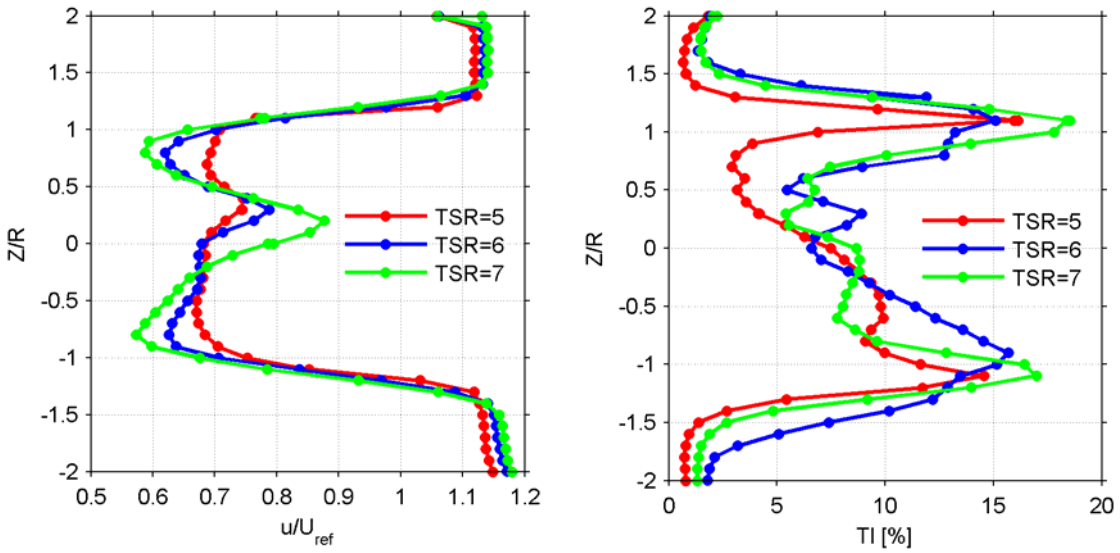

Fig. 28. Normalized mean velocity u/Uref [-] and turbulence intensity TI [-]at 3D distance behind T_1 – low turbulent flow.

In Fig. 28 the mean velocity is shown for 3D distance downstream of the first turbine operating in three different tip-speed ratios. In 3D distance there are noticeable regions behind end of the blades, where velocity is much lower than in the hub area. Rise of the differences in velocity between the wake in the hub area and end of the blades rise with TSR growth. Moreover, asymmetry of the wind distribution is measurable.

As it was expected, the lowest wind velocity was measured for TSR=7 and it is u/U_{ref}=0.57 because of higher blockage effect generated by the turbine working in higher RPM.

Performance of turbulence intensity was also various in hub area and near the rotor edge. Furthermore, differences between them were up to 13%.

As it was expected, the highest turbulence intensity was measured when T_1 was working in the highest TSR and maximum value is TI=18.56%. Unexpectedly, maximal TI point for TSR=5 was slightly higher than for TSR=6 than it was assumed. Even though, it was only one point which is shifted. Rest of the curve has clearly lower turbulence intensity than for TSR=6. The most possible explanation of this phenomenon is a measurement error and slightly different inlet condition in each experiment.

3D distance

real TSR	mean U_{ref} [m/s]	min. u [m/s]	min. u/U_{ref} [-]	max. u/U_{ref} [-]	min. TI (hub area)	max. TI [%]
4.94	11.6	7.76	0.671	1.15	2.93	16.1
5.95	11.5	7.15	0.620	1.17	5.46	15.7
6.90	11.5	6.59	0.574	1.18	5.40	18.5

Table. 2. Summary of the results from 3D distance horizontal wake measurements – low turbulence.

- 5D distance

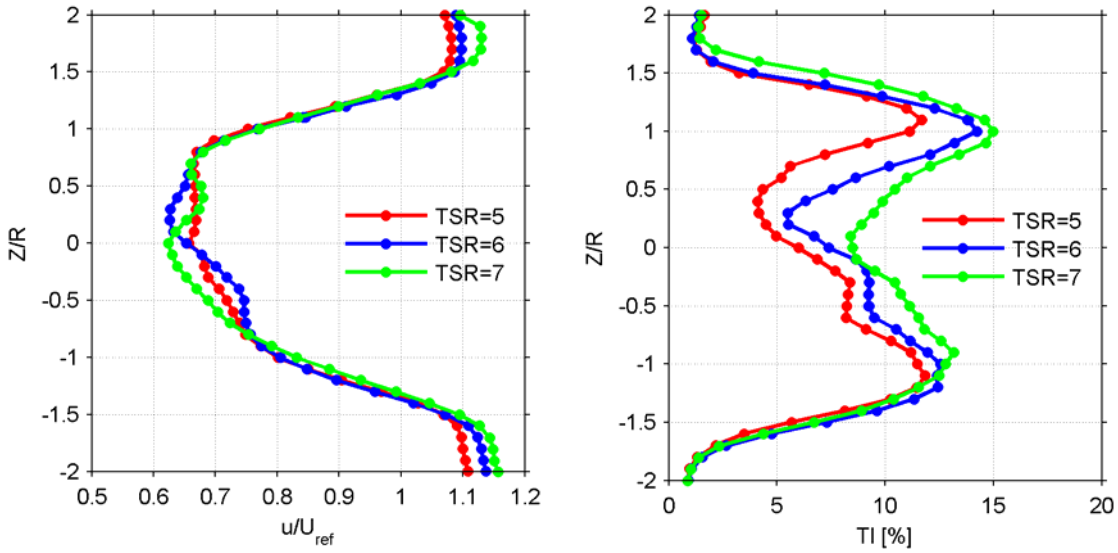

Fig. 29. Normalized mean velocity u/Uref [-] and turbulence intensity TI [-]at 5D distance behind T_1 – low turbulent flow.

At the distance of 5D downstream of the first turbine velocity differences at various TSR were not as high as it was observed at 3D distance and What is more, the highest velocity deficit was found for TSR=7 and it was u/U_{ref}= 0.62. Each TSR had small displacement area but it was noticeable only in the hub area and in free unobstructed stream far from the rotor.

In spite of the fact that there were no big differences in wake velocity between different TSR test cases, still the turbulence intensity profile of each wake has similar behavior as it was in previous distance. The highest TI=15% was connected with TSR=7, but in that case the differences between max and min value is less than it was at 3D case.

5D distance

real TSR	mean U_{ref} [m/s]	min. u [m/s]	min. u/U_{ref} [-]	max. u/U_{ref} [-]	min. TI (hub area)	max. TI [%]
5.11	11.5	7.55	0.658	1.11	4.11	11.8
6.09	11.5	7.18	0.626	1.14	5.49	14.2
6.92	11.5	7.16	0.624	1.16	8.40	15.0

Table. 3. Summary of the results from 5D horizontal wake measurements – low turbulence level.

- 8.5D distance

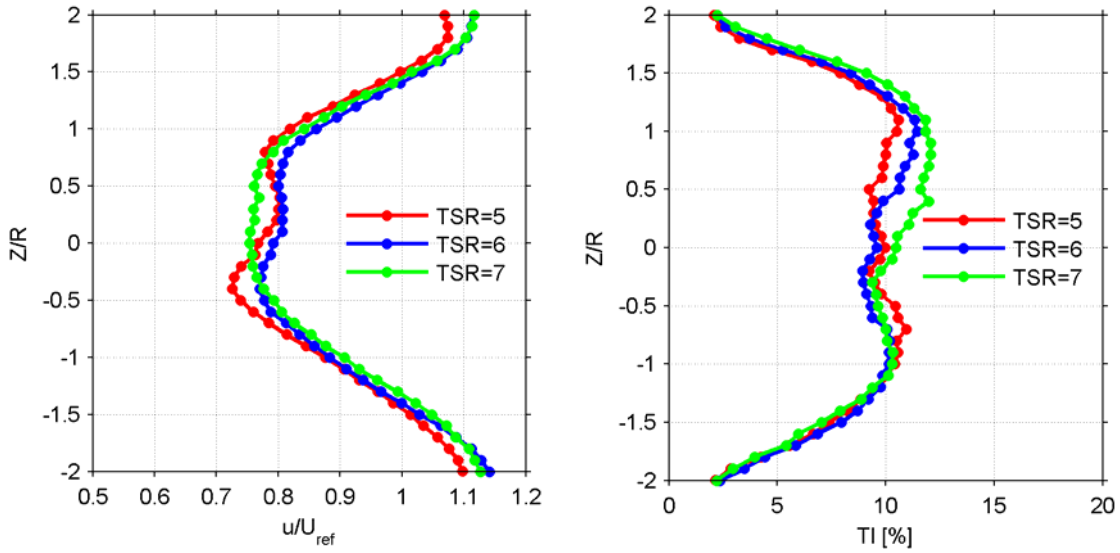

Fig. 30. Normalized mean velocity u/Uref [-] and turbulence intensity TI [-]at 8.5D distance behind T_1 – low turbulent flow.

The 8.5D distance wake behind the turbine is the most interesting one for two reasons.

First of all, no-fully recovered flow was observed at 8.5D distance wake measurement. Although, both mean velocity and turbulence intensity reached similar level independently of the TSR and the velocity deficit is much reduced than in closer distances (3D, 5D). There was still slight difference between hub area and area near the end of the rotor. Moreover, area of reduced velocity was much smaller than rotor of the turbine

On the other hand, following measurements were provided in the end of the wind tunnel and HW probe was under traverse mechanism. It means that velocity measured in last experiment could be influenced by smaller cross-section of the tunnel and results could be overestimated.

This explanation could be confirmed by experiment made with second turbine to check operation parameters with and without traverse system. Unfortunately it was not confirmed as the results with traverse system above the turbine have been relatively higher than without it. Besides, it is still matter of discussion how big influence caused traverse system on this experiment.

Furthermore, next wake measurements were made without automatic traverse mechanism to be sure that wake is not influenced.

8.5D distance

real TSR	mean U_{ref} [m/s]	min. u [m/s]	min. u/U_{ref} [-]	max. u/U_{ref} [-]	min. TI (hub area)	max. TI [%]
5.06	11.4	8.30	0.725	1.10	9.22	11.0
6.04	11.4	8.78	0.770	1.14	8.95	11.4
7.00	11.4	8.59	0.753	1.13	8.88	12.1

Table. 4. Summary of the results from 8.5D horizontal wake measurements – low turbulence.

6.3.2 High turbulence intensity stream flow

- 3D distance

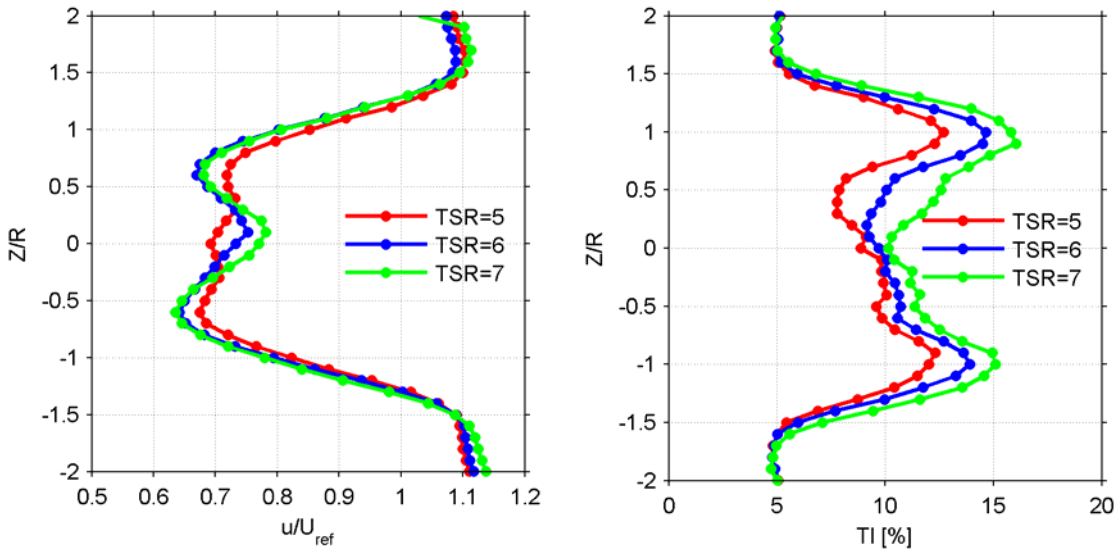

Fig. 31. Normalized mean velocity u/Uref [-] and turbulence intensity TI [-]at 3D distance behind T_1 – high turbulent flow.

Wake distribution behind first turbine operating in high turbulence flow has significantly different shape than it was when turbulence was low.

It was expected that differences between velocity profiles of each TSR of T_1 will be much higher than it was observed after analyzing the data. Moreover, regions with the highest velocity deficit were much closer to the axis of turbine, near of the half of the rotor radius. In experiments with low turbulent inlet flow (3D distance) area of reduced velocity was seen near the blades edge. The lowest velocity in the wake was characteristic for TSR=7 and it was $u/U_{ref} = 0.637$, but variance among other TSR values was marginal.

Turbulence intensity at this point was more similar to previous measurements (low turbulent inlet flow). There were still noticeable changes of TI for each TSR of T_1 but they were much smaller than in previous case at the same distance.

3D distance

real TSR	mean U_{ref} [m/s]	min. u [m/s]	min. u/U_{ref} [-]	max. u/U_{ref} [-]	min. TI (hub area)	max. TI [%]
4.89	11.44	7.71	0.674	1.11	7.77	12.7
5.90	11.44	7.34	0.642	1.12	9.14	14.7
6.92	11.49	7.31	0.637	1.14	10.1	16.0

Table. 5. Summary of the results from 3D horizontal wake measurements – high turbulence.

- 5D distance

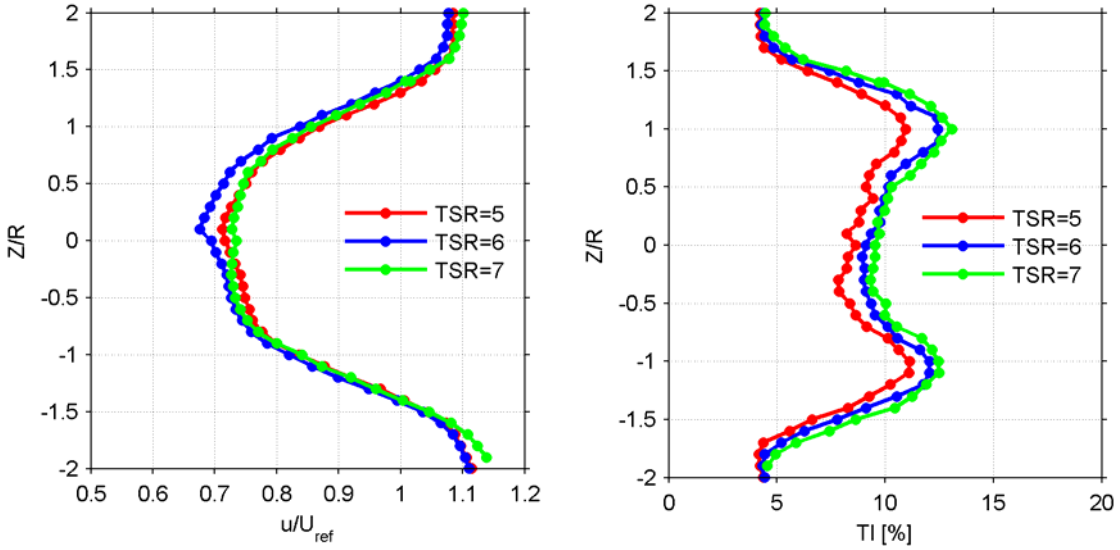

Fig. 32. Normalized mean velocity u/Uref [-] and turbulence intensity TI [-]at 5D distance behind T_1 – high turbulent flow.

In this experiment the velocity profiles of each TSR were similar. The lowest value u/U_{ref}=0.676 was reached when turbine has been operated in TSR=6, but it seems to be coincidence connected with measurement error or specific measurement technique than real lower velocity measured exactly in this operation point. Nevertheless, velocity profiles are comparable and error like that is negligible. There was no velocity growth seen at the center of the rotor area at it was in all previous experiments.

Turbulence intensity at 5D distance has still noticeable peaks in the profile. There is big recovery tendency observed and the biggest difference in TI between lowest value around the hub area and near the rotor edge was around 4%.

5D distance

real TSR	mean U_{ref} [m/s]	min. u [m/s]	min. u/U_{ref} [-]	max. u/U_{ref} [-]	min. TI (hub area)	max. TI [%]
4.82	11.5	8.20	0.712	1.11	7.84	11.1
5.81	11.5	7.79	0.676	1.11	8.85	12.5
6.77	11.47	8.33	0.727	1.14	9.32	13.0

Table. 6. Summary of the results from 5D horizontal wake measurements – high turbulence.

- 8.5D distance

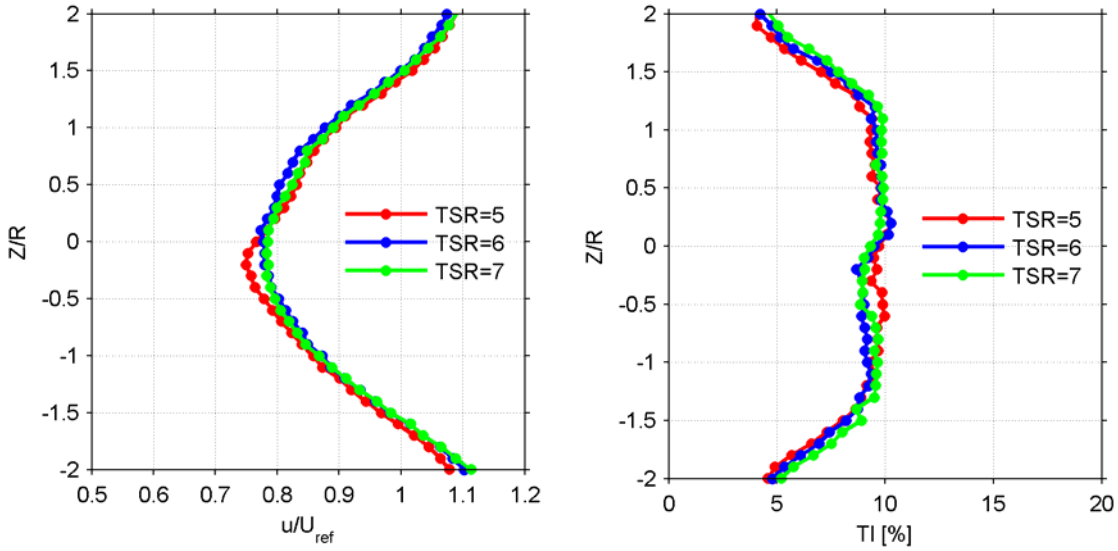

Fig. 33. Normalized mean velocity u/Uref [-] and turbulence intensity TI [-]at 8.5D distance behind T_1 – high turbulent flow.

The velocity profiles at 8.5D downstream of first turbine has been also not fully recovered. Profiles of particular TSR has followed the same line. Recovery of the velocity from previous distance was around 0.1 u/U_{ref} .

Furthermore, intensity of turbulence was fully stable at the area swept by the turbine rotor for all three TSR used in this experiment. Maximal value reached at TI=10.3% both for TSR=5 and for TSR=6.

8.5D

real TSR	mean U_{ref} [m/s]	min. u [m/s]	min. u/U_{ref} [-]	max. u/U_{ref} [-]	min. TI (hub area)	max. TI [%]
4.90	11.5	8.62	0.750	1.09	8.89	10.3
5.78	11.5	8.89	0.773	1.10	8.20	10.3
6.89	11.5	8.99	0.782	1.11	8.84	9.91

Table. 7. Summary of the results from 8.5D horizontal wake measurements – high turbulence.

6.3.3 Review of horizontal wake experiments

Comparison of the horizontal wake measurements is presented below. Figures from 34 to 37 gives an overlook of velocity deficit and turbulence intensity distribution evolving along the separation distance from the turbine.

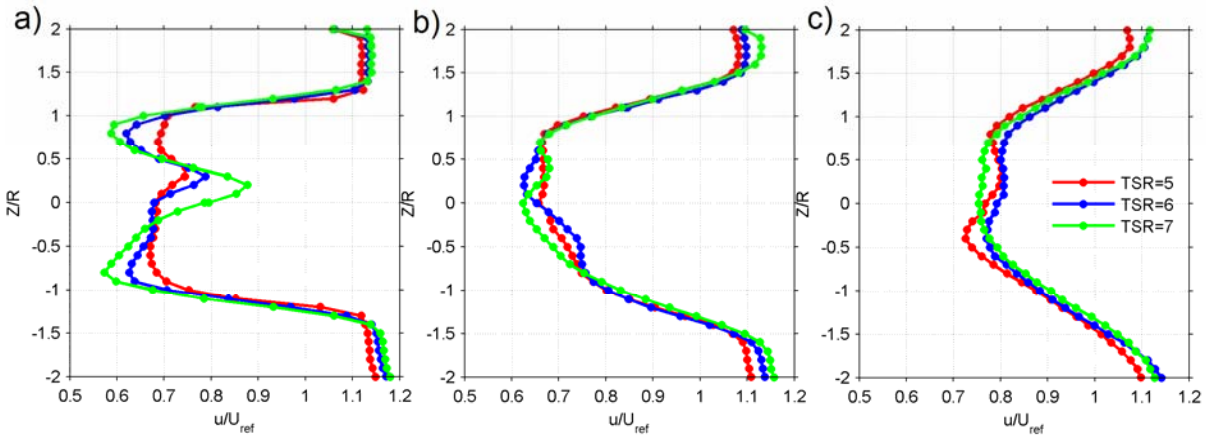

Fig. 34. Horizontal axis normalized mean velocity u/Uref [-] between two model wind turbines at a) 3D, b) 5D, c) 8.5D behind T_1 operating in low turbulent inlet flow.

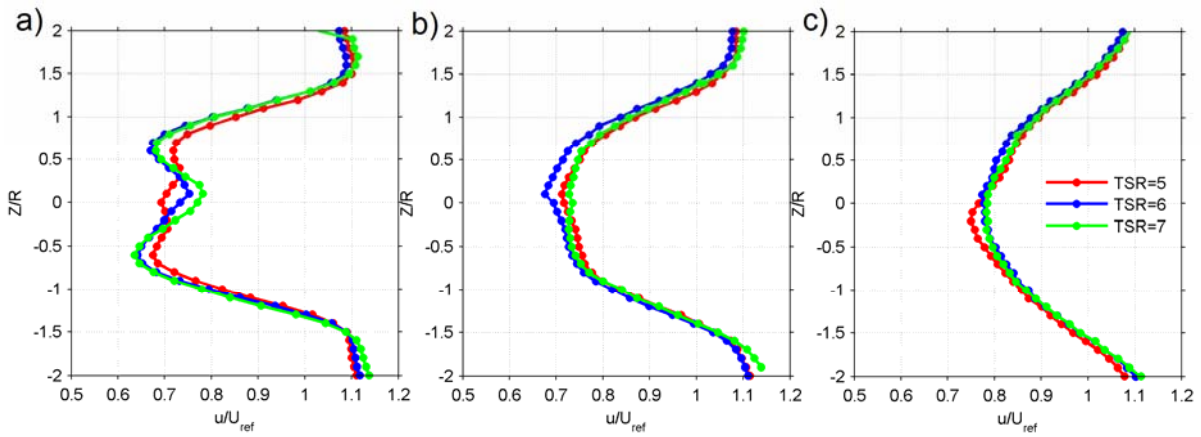

Fig. 35. Horizontal axis normalized mean velocity u/Uref [-] between two model wind turbines at a) 3D, b) 5D, c) 8.5D behind T_1 operating in high turbulent inlet flow.

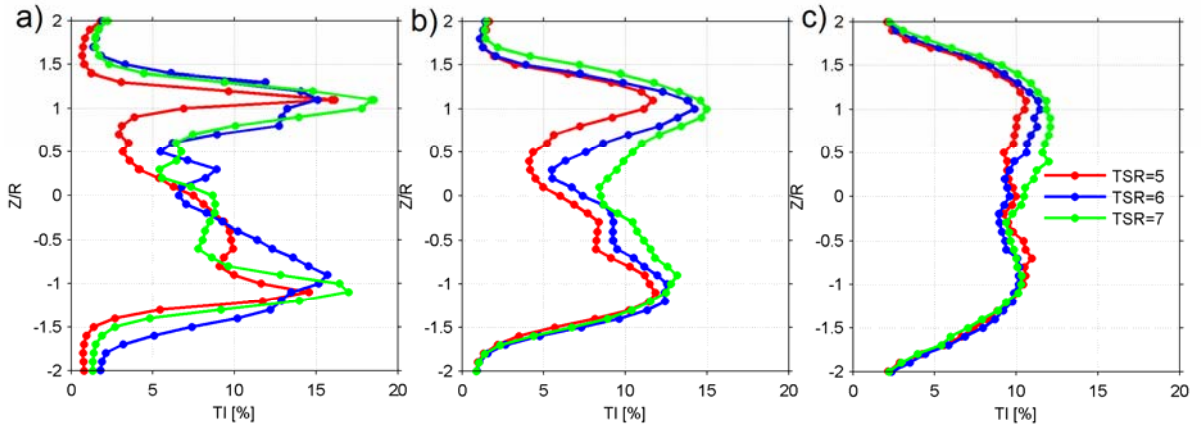

Fig. 36. Horizontal axis turbulence intensity TI [%] between two model wind turbines at a) 3D, b) 5D, c) 8.5D behind T_1 operating in low turbulent inlet flow.

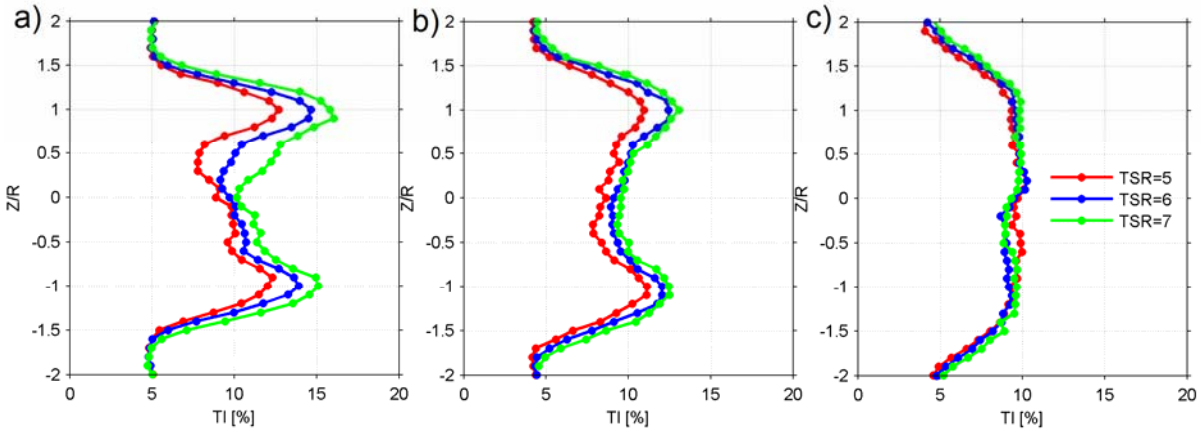

Fig. 37. Horizontal axis turbulence intensity TI [%] between two model wind turbines at a) 3D, b) 5D, c) 8.5D behind T_1 operating in high turbulent inlet flow.

After deep analysis of the preceding results from horizontal wake measurements behind single turbine with low and high turbulent flow at 3D, 5D and 8.5D downstream, few main deductions might appear:

- The wake of the turbine has been recovering along the downstream distance. Results from unobstructed flow had been characterized with high differences in mean velocity between center of the wake and area of the rotor edge. Turbine operated in high turbulent flow had significantly lower characteristic of the velocity differences.

- Minimal values of velocity for each distance were comparable but still they were slightly higher for higher turbulence inflow (when the grid was mounted in the test section) than without it. At TSR=5 and TSR= 6 it was 4% of difference and at TSR=7 it was 10% of difference. Nevertheless, more important parameter is width of the wake, which was wider in turbulent flow but provided much higher velocity in the edge of the blades.

- As it was expected, the center of the wake had the tendency to displace from the hub axis. This phenomenon was detected and investigated in previous publications for instance [29,30, 36, 41]. Only in high turbulent inlet flow at 5D distance and 9D distance this phenomenon had been reduced.

- The higher velocity region was observed outside 1.5 radius from the rotor axis. Velocity on the left and right side was higher (up to 18%) than steady reference velocity. This fact was related to blockage effect caused by working turbine. It was also found in previous similar researches [29,30, 36, 41]

- Tip-speed ratio close to the optimal (5-7) has negligible influence on the velocity profile shape. Only in closer regions like 3D the impact of TSR was considerable.

- Turbulence intensity is not depended on velocity profile. Velocity profile in the wake was shrinking along the distance behind the turbine. However, turbulence intensity profile was not corresponding to the velocity profile and its width was steady along the downstream. This phenomena is observed both in low and high turbulent flow.

- The highest turbulence intensity differences were noticed in the wake behind turbines working in unobstructed stream. There was decreasing tendency observed along the tunnel. For 8.5D distance behind both for the grid and no grid conditions turbulence intensity profile was fully expanded at rotor area and stood at approx. 10%.

- Measurements made at 8.5D downstream could be overestimated by reason of smaller cross-section of the wind tunnel. The HW probe was mounted under automatic traverse mechanism because of lack of space in the test section. This situation might have influence of the results.

6.4 Vertical wake development between two wind turbines

This chapter is devoted to present and analyze wind velocity profile expansion along the downstream distance. Measurements were made by vertical manual traverse system at 3D, 5D, 8D distance behind the first turbine, when the second turbine was mounted and at 9D distance. Additionally, the wake at 9D position, was done when second turbine was taken out.

As it was in previous experiments also here two cases were investigated. One, where low turbulence intensity was used in the inlet stream and second one, with high turbulence inlet stream.

First turbine was always working at TSR=6.0, which was optimal, designed value. Second turbine tip speed ratio was established as TSR=5.0, where the best efficiency was found in the wake.

Main aim of this experiment was to investigate the influence of the second turbine performance on the wake upstream. Surprisingly, each setup with different TSR of T_2 gave exactly the same results, even at 1D before the turbine. For that reason this set of experiments can be treated like a vertical turbulence intensity measurements behind T_1 only.

6.4.1 Low turbulence intensity stream flow

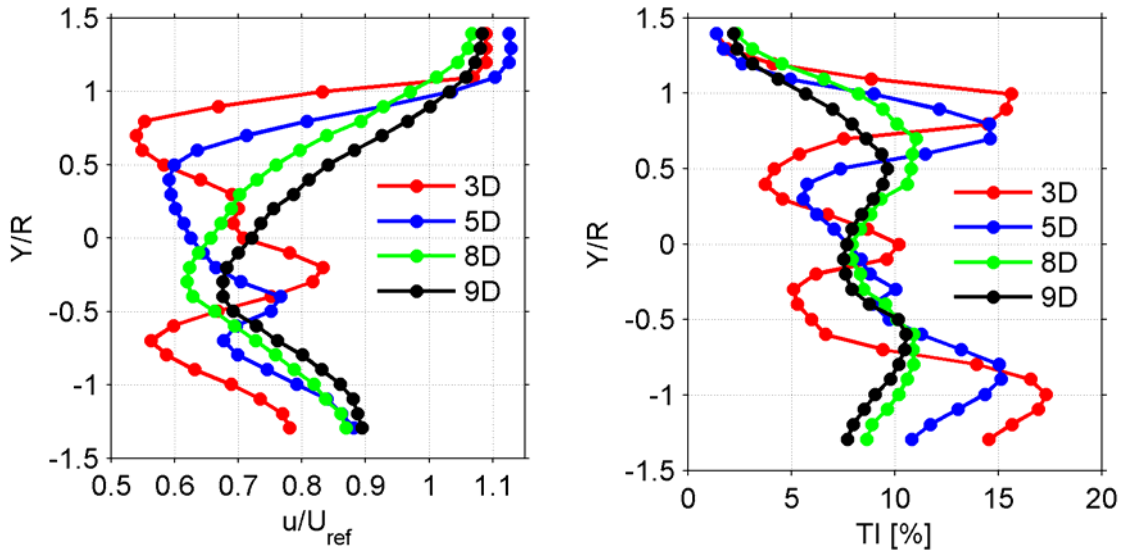

Fig. 38. Normalized mean velocity u/Uref [-] and turbulence intensity TI [-]. Parameters: T_1 TSR=6.0; T_2 TSR=5.0. Vertical wake – low turbulent flow

Results of the wake measurements are plotted on Fig. 38. and the most important parameters are shown in the table 8. below. The first thing noticed after the analyses was the movement of center of the wake. First two curves at 3D and 5D distance had noticeable downward movement, also in case where tip vortices areas were observed, 94 mm downward on first distance and 188 mm at 5D. For next two distances, the tip vortices had been not observed and centre of the wake at 8D distance was on the same level as at 5D and at 9D was 47 mm lower than before.

As it was expected the biggest velocity deficit had been found in the closest distance near the first turbine and the slight increase along the distance was observed.

Turbulence intensity profile shape for first two steps (3D and 5D distance) were possible to guess, that differences of each setup would be significant. However, only profiles at 8D and 9D distances were represented by almost similar curve. There was observed only negligible mismatch (around 2.5%) on the upper part of the wake, which had the beginning above Y/R=0.4 distance from the rotor center. Rest of the parameters of each setup are presented in table 8.

T_1 TSR=6.0

Distance	real TSR	mean U_{ref} [m/s]	min. u [m/s]	min. u/U_{ref} [-]	max. u/U_{ref} [-]	min. TI (hub area)	max. TI [%]
3D	6.00	11.5	6.22	0.540	1.10	3.74	17.3
5D	6.00	11.5	6.80	0.591	1.13	5.57	15.1
8D	6.01	11.5	7.12	0.619	1.07	7.91	11.0
9D	6.00	11.5	7.77	0.675	1.08	7.52	10.5

Table. 8. Summary of the results from vertical wake measurements – low turbulence

6.4.2 High turbulence intensity stream flow

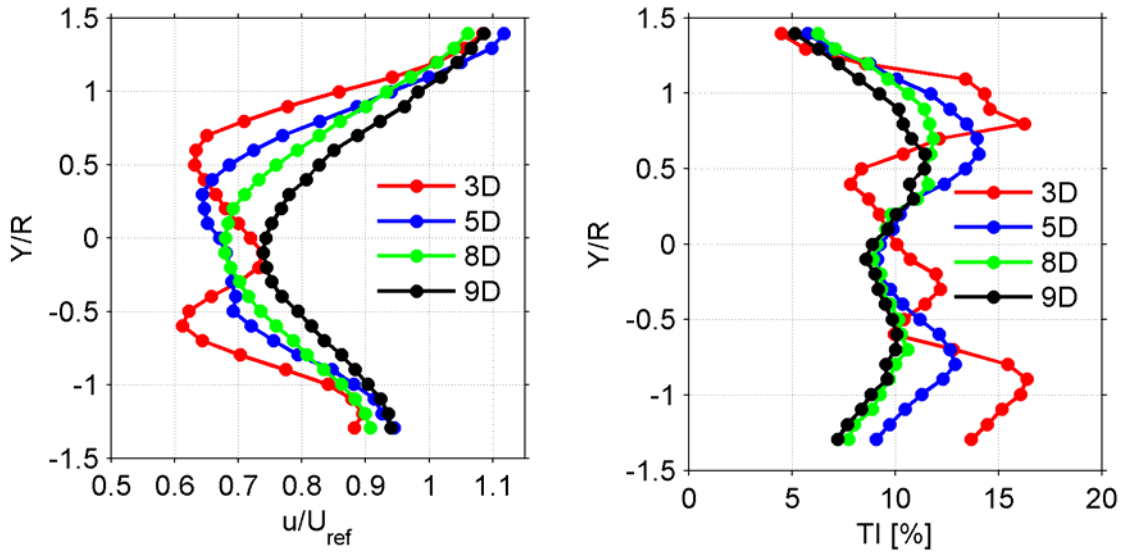

Fig. 39. Normalized mean velocity u/Uref [-] and turbulence intensity TI [-]. Parameters: T_1 TSR=6.0; T_2 TSR=5.0. Vertical wake – high turbulent flow

Fig. 39 shows results of turbulence intensity measurements after the experiment with high turbulent inlet flow. As it was seen in low turbulent inlet flow wake tests, in current case the observed downward movement of the wake was noticed, but it was not so intensive. Maximal movement was observed at 3D distance and it was 94 mm.

Furthermore, turbulence intensity has reached similar or lower values than for previous case with low turbulent stream. What is more, also here it was observed that the difference in TI between profiles at 8D and at 9D. It started to be noticeable for the location above Y/R=0.6 from the rotor axis and it was not more than 1.4%.

Important mismatch with previous experiments is higher reference velocity (11.7 m/s instead of 11.5 m/s).

T_1 TSR=6.0

Distance	real TSR	mean U_{ref} [m/s]	min. u [m/s]	min. u/U_{ref} [-]	max. u/U_{ref} [-]	min. TI (hub area)	max. TI [%]
3D	5.90	11.7	7.17	0.613	1.11	7.83	16.4
5D	5.90	11.7	7.54	0.644	1.15	9.10	14.1
8D	5.90	11.7	7.94	0.678	1.08	8.93	11.8
9D	5.90	11.7	8.66	0.740	1.09	8.57	11.5

Table. 9. Summary of the results from vertical wake measurements – high turbulence

6.4.3 Review of vertical wake experiments

This chapter is devoted to summarize the vertical wake measurements of the low and high turbulent in let flow. Figures 40 – 43 show velocity deficit and turbulence intensity development at the next positions of traverse.

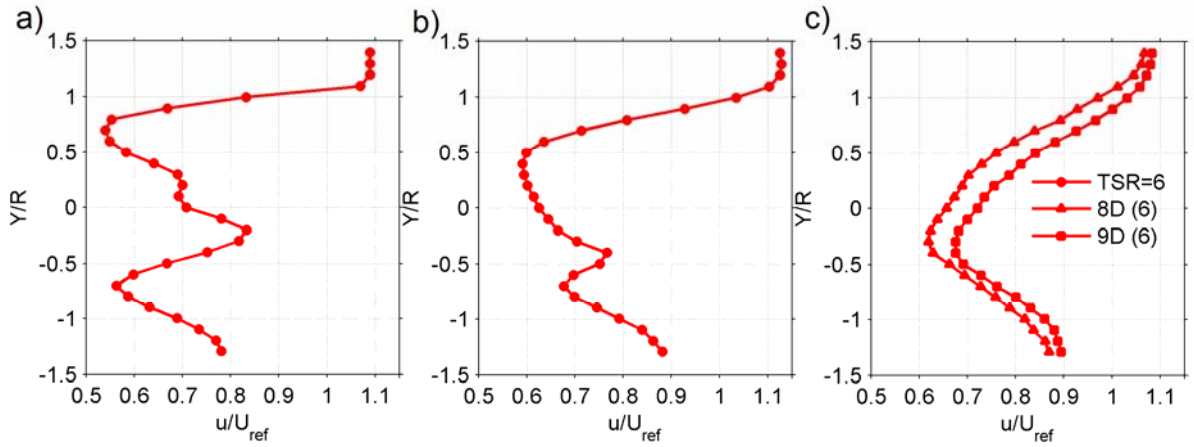

Fig. 40. Vertical axis normalized mean velocity u/Uref [-] between two model wind turbines at a) 3D, b) 5D, c) 8D and 9D behind T_1 operating in low turbulent inlet flow. Parameters of the turbines: T_1 TSR=6.0; T_2 TSR=5.0.

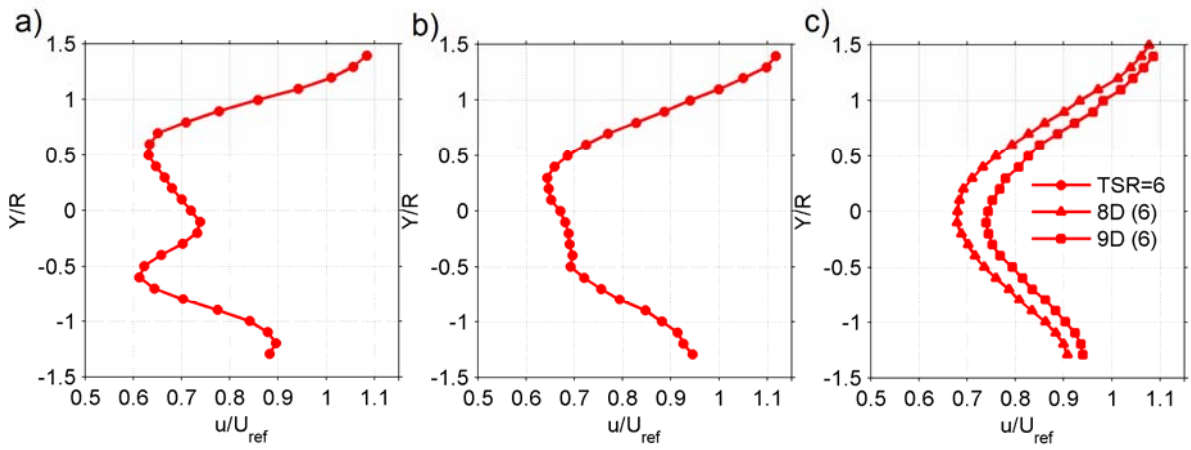

Fig. 41. Vertical axis normalized mean velocity u/Uref [-] between two model wind turbines at a) 3D, b) 5D, c) 8D and 9D behind T_1 operating in high turbulent inlet flow. Parameters of the turbines: T_1 TSR=6.0; T_2 TSR=5.0.

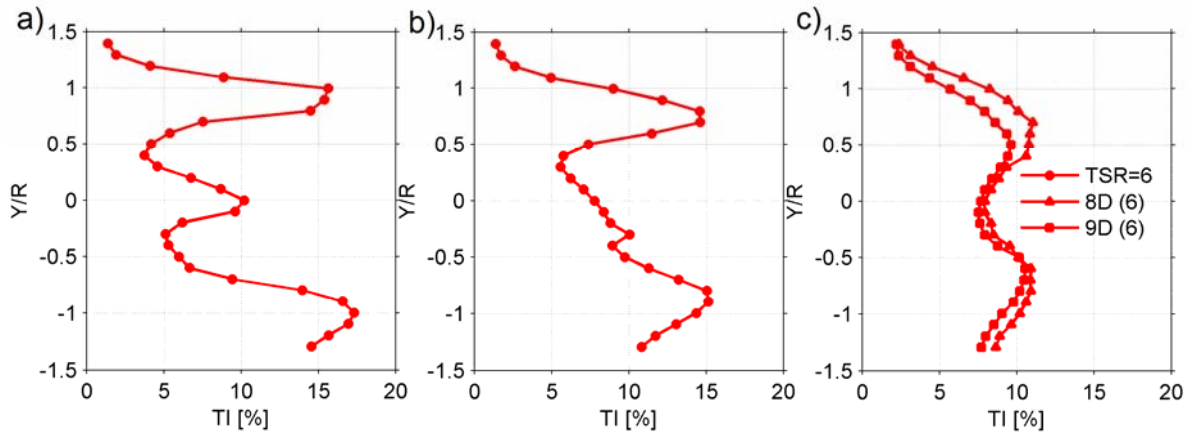

Fig. 42. Vertical axis turbulence intensity TI [%] between two model wind turbines at a) 3D, b) 5D, c) 8D and 9D behind T_1 operating in low turbulent inlet flow. Parameters of the turbines: T_1 TSR=6.0; T_2 TSR=5.0.

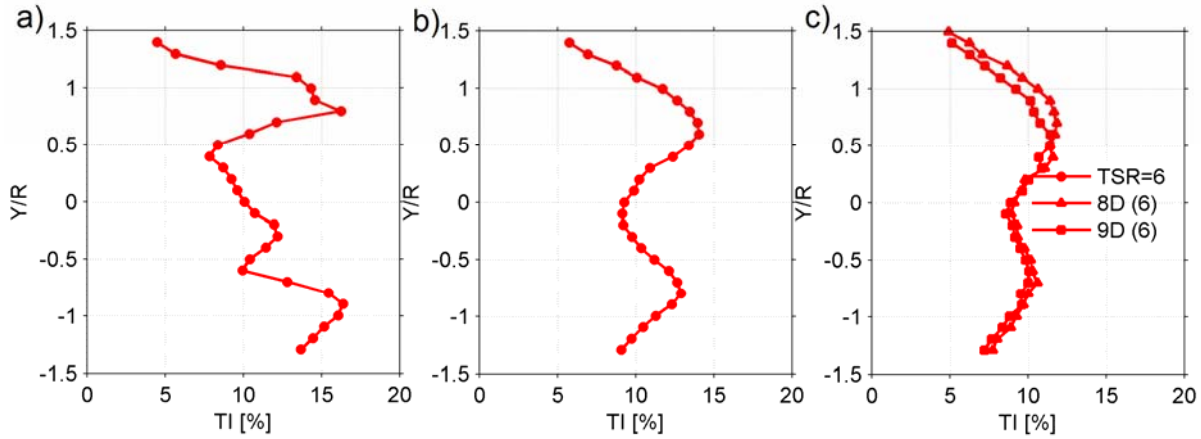

Fig. 43. Vertical axis turbulence intensity TI [%] between two model wind turbines at a) 3D, b) 5D, c) 8D and 9D behind T_1 operating in high turbulent inlet flow. Parameters of the turbines: T_1 TSR=6.0; T_2 TSR=5.0.

As a result of examination of vertical wake profiles for low and high turbulent inlet stream flow in the middle of two operating turbines, the following assumptions were made:

- Wake profile in low and high turbulent flow has unsymmetrical shape. The thick tower of the turbine has influenced the wake on the bottom side of the flow. Effect of the tower obstruction was reduced on high turbulent inlet stream.

- Low turbulent flow was characterized by lower speed of velocity recovery along the downstream. Minimal mean dimensionless velocity was approx. 10% smaller than in turbulent flow, but this phenomenon is probably caused by higher reference velocity.

- 9D distance vertical profile velocity measurements were made, while T_2 was not inside the test section for evaluation of tandem setup performance. . Results of TI intensity in this case are comparable and velocity profile shows no differences to expected and obtained for two turbine case.

- Turbulence intensity of high and low turbulent inlet stream had smoother profile in comparison for each distance. The biggest difference was noticed in the centre of the wake and it was declining on the edges of rotor area.

- Experiments with the grid shows different turbine performance at different inlet turbulence intensity levels. There was noticeable displacement of turbulence intensity profile in downward area caused by the tower aerodynamic shadowing. This phenomenon was more visible for low turbulence intensity inflow (without the grid).

7 Conclusions

Power measurements prove foregoing expectations of possibility of finding the optimal power output of the wind farm by modifying tip-speed ratio at the same wind velocity. Moreover, additional investigated cases with high and low turbulent inlet flow and different separation distance between inline arrayed turbines confirmed existence of such optimal conditions. Turbine operated in the wake of the first turbine produces less energy - reduction of tip-speed ratio of the first, wake generating turbine, causes smaller decrease of the wind velocity behind it. This phenomenon is translated into increase of energy extracted from the second turbine and more important into increase of total energy extracted by two turbines.

Depending on the separation distance, in laminar inflow case, the total (for two turbines) power production increase, by 10.7% to 4.08% compared to turbines operating at individual design parameters (TSR). Power growth was also noticeable in high turbulent inlet stream, reaching the increase between 2.09% on 9D to 9.49% at 3D compared to suboptimal operating case. In laminar flow case, the first turbine tip-speed ratio was varied between 4.0 and 6.5 when in turbulent it was kept steady at TSR= 6.0 to reach the peak. Thus, the second turbine rotor rotation had been reduced to TSR=4.0-5.0.

The separation distance between the turbines has also significant influence on power production. In laminar flow case, the second turbine had been moved from 3D to 5D behind the first one, what gave 5.9% higher power output than in previous setup (3D distance). Moreover, further movement to 9D caused additional growth of 14.6%. Similar behavior could be found for turbulent inlet stream. First turbine displacement gave 7.5% more power than at 3D separation distance. Next position at 9D of second turbine was characterized by 13.6% higher power coefficient than at 5D distance.

Furthermore, even inlet wind conditions affected power generation of the turbine tandem. Comparison measurements with the turbulence promoting grid at the inlet with measurements of unobstructed stream revealed power outcome higher by 5.0% - 6.7% in favor of turbulent inflow. That can be explained by different shape of the velocity deficit profile at the T_1 wake.

Performed wake measurements allow to compare results of power coefficient measurements, draw conclusions and additionally explain them from aerodynamic point of view.

First of all, horizontal axis measurements were done on the rotor hub height only behind one turbine. Differences in the wake velocity at operating tip speed ratio TSR 5 – 7 have been significant only at the distance 3D downstream after the rotor. Although, turbulence intensity profiles had reached similar level only at 5D and 8.5D distance for turbulent inflow.

In external area of the rotor edge the 18 % increase of velocity comparing to reference in all of wake measurements was observed. This phenomenon was caused by blockage effect of the turbine – cross section of the operating rotor is to high for the cross section of the wind tunnel. Due to fact of the turbine blockage, it is possible that results connected with Cp might be overestimated in relation to full scale wind turbines.

After comparison of wake measurements with power measurements it was observed that combination of higher turbulence intensity at the inlet stream increased power output of the second turbine. Higher turbulence in area swapped by the rotor should cause reduction of gained power, but on the other hand this phenomenon caused fester recovery of the downstream flow filed. Minimal velocity was at the comparable level of the wake at laminar and turbulent inlet flow for each separation distance, but velocity at rotors edge was noticeably higher, which was most important for final power output.

Vertical wake measurements between two turbines showed that there is no measurable influence of the second turbine on an upstream wake generated only by first turbine in a row. The difference in turbulence intensity and velocity deficit was not observed, even at 1D distance in front of the second turbine rotor.

Comparison of vertical and horizontal wake made possible to see that velocity deficit area have been shrinking much faster on upright direction than horizontal. Moreover, there was observed high downward movement of the wake from the center and lower half of the profile was highly affected by the thick turbines tower. Center of the turbulence intensity profile had also tendency to downward axial movement, even though the TI profile has not been shrinking along the distance and what is more, the turbines tower did not affect the lower part of the profile (accept close distance 3D with low turbulent inlet flow).

Analyzing wake measurements there could be also concluded that recovery of the wake was more noticeable on measurements in horizontal direction than in vertical. This phenomenon is

probably connected with difference of the width and height of the tunnel. The tunnel is much wider, so wake expansion is less affected by the tunnel walls. Unsymmetrical wake expansion and also movement of the wake in downward and right direction was also responsible for higher efficiency of the turbine operating in far wake.

To sum up, the total power output increase is one of the main tasks for designing and upgrading ng the wind farms and hopefully this measurements data will be used as a one of ways to improve simulation models. Improvement of output of the two arrayed turbines tested in laboratory conditions was significant. When the turbines were spaced by 3D distance from each other and they were working at their designed TSR, power coefficient of the turbines tandem reached Cp=0.536, but after using all described corrections moving the output towards optimal, the synergic effect of optimization of TSR, TI inlet and separation distance allowed for reaching Cp=0.762 what was 42.2% increase compared with typical case.

8 Future work

In this project a lot of data connected with optimization of total power generation of the two in-line model scale wind turbines was collected. Only few cases to reach the optimum were investigated, for instance different separation setup, low and high turbulent flow and TSR adjustment. One of idea of this project was to check how big impact on total power production can be increased if efficiency of first turbine will be reduced. After obtaining the promising results of this method there are few possible ways to get more data with small modification of the set up or just to find better efficiency of the laboratory wind farm.

Few ideas that may be interesting to investigate as a continuation of existing work are shown below:

- A shear-flow grid can be used to check and compare efficiency when inlet parameters are closer to natural (boundary layer).
- Different or additional way of reducing energy extraction at first turbine can be used. For instance, parameters like yaw angle of the turbine or pitch angle of the blades can be also modified.
- The pitch angle modification of the second turbine blades can be also promising, especially when there was found that operating in full wake require the setup different than optimal.
- The two turbines optimization with whole previous modifications, but when the turbines are shifted. It means that the second turbine is operating in semi-wake zone.

As it was shown above, there are numerous possibilities of how to find the best total power coefficient for the two turbines. What is more, for each setup, the wind performance behind one or two turbines should be also investigated. Those experiments for sure would answer many questions and what is more, they could encourage modelers to update their simulation techniques and wind farm owners to better use of the already existing turbines.

Bibliography

[1] *Iowa Energy Center – History of Wind Energy* [Online, 2014, Aug] http://www.iowaenergycenter.org/wind-energy-manual/history-of-wind-energy/

[2] *Illustrated History of Wind Power Development* [Online, 2014, Aug] http://www.telosnet.com/

[3] S. Emsie, *Wind Energy Meteorology*, Springer-Verlag, Berlin Heidelberg 2013

[4] *World Wind Energy Association* [Online, 2014, Aug] http://wwindea.org/home/index.php?option=com_content&task=view&id=421&Itemid=43

[5] *World Wind Energy Association – Key statistics of World Wind Energy Report 2013*, Shanghai, 7 April 2014 [Online, 2014, Aug] http://www.wwindea.org/webimages/WWEA_WorldWindReportKeyFigures_2013.pdf

[6] *World Wind Energy Association* – Quarterly Bulletin, June 2014 [Online, 2014, Aug] http://wwindea.org/webimages/WWEA-QB-2-20140805.pdf

[7] SYMKOM conference, Lodz, 2014

[8] J. Højstrup, *Spectral coherence in wind turbine wakes*. Journal of Wind Engineering and Industrial Aerodynamics, 80:137–146, 1999

[9] A. P. Martins, P. C. Costa, A. S. Carvalho, *Coherence and wakes in wind models for electromechanical and power systems standard simulations*. EWEC conference, Athens, 2006

[10] L.J. Vermeera, J.N. Sorensen, A. Crespo, *Wind turbine wake aerodynamics*, Progress in Aerospace Sciences, 2003

[11] J. Å. Dahlberg. *Assessment of the Lillgrund Windfarm: Power performance, wake effects.* Technical report. The Swedish Energy Agency, September 2009

[12] B. Sanderse, *Aerodynamics of Wind Turbine* Wakes, ECN, literature review 2009

[13] T. Burton, D. Sharpe, N. Jenkins, E. Bossanyi, *Wind Energy Handbook,* Second edition, Wiley, 2011

[14] E. Hau, *Wind Turbines – Fundamentals*, Third edition, Springer-Verlag, Berlin Heidelberg, 2013

[15] J. F. Maxwell, J. G. McGowan, *Wind Energy Explained,* Second edition, Willey, 2009

[16] M. Ragheb, A. M. Ragheb, *Wind turbines theory*, University of Illinois at Urbana Champaign, USA, 2011

[17] M.-K. Liu, M.A. Yocke, T.L. Myers. *Mathematical model for the analysis of wind turbine wakes*. *Journal of Energy*, 7:73–78, 1983

[18] Massachusetts Institute of Technology [Online, 2014, Sep] http://www.mit.edu/course/1/1.061/OldFiles/www/dream/SEVEN/SEVENTHEORY.PDF

[19] CFD Online [Online, 2014, Oct] http://www.cfd-online.com/Wiki/Turbulence_intensity

[20] J.W. Cleijne, *Results of Sexbierumwind farm; single wake measurements*. Technical Report TNO-Report 93-082, TNO Institute of Environmental and Energy Technology, 1993

[21] Popular Science [Online, 2014, Oct] http://www.popsci.com/technology/article/2010-01/wind-turbines-leave-clouds-and-energy-inefficiency-their-wake

[22] R.J. Barthelmie, S.T. Frandsen, K. Hansen, J.G. Schepers, K. Rados,W. Schlez, A. Neubert, L.E. Jensen, and S. Neckelmann. *Modelling the impact of wakes on power output at Nysted and Horns Rev*. In European Wind Energy Conference, 2009

[23] M. Samaroni*, Handbook of Wind Power Systems – The Wind Farm Layout Optimization Problem*, Springer-Verlag, Berlin Heidelberg, 2013

[24] L. Chamorro, F. Porte-Agel, *Effects of Thermal Stability and Incoming Boundary- Layer Flow Characteristics on Wind Turbine Wakes: A Wind-Tunnel Study*. Boundary Layer Meteorology, 515-533, 2010a

[25] L. Chamorro, R. Arndt, F. Sotiropoulos, *Turbulent flow properties around a staggered wind farm*. Boundary - Layer Meteorology, 349-367, 2011

[26] M. Adaramola, P. Krogstad, *Experimental Investigation of wake effects on wind turbine performance*. Renewable Energy, 2011

[27] K.E. Johnson, N. Thomas, *Wind farm control: addressing the aerodynamic interaction among wind turbines,* American Control Conference; St. Louis, MO, USA, 2009

[28] P. Krogstad, P. E. Eriksen *"Blind test" calculations of the performance and wake development for a model wind turbine,* Renevable Energy, 2013

[29] F. Pierella, P. Krogstad, L. Saetran, *Blind Test 2 calculations for two in-line model wind turbinek*, Renevable Energy, 2013

[30] P. Krogstad, L. Saetran , M. S. Adaramola, *"Blind test" calculations of the performance and wake development behind two in-line and offset model wind turbines*, Renevable Energy, 2015

[31] Norwegian University of Science and Technology webside [Online, 2014, Nov] http://www.ivt.ntnu.no/mekanikk/Vindtunell.htm

[32] Politecnico di Milano official webside [Online, 2014, Nov] http://www.windtunnel.polimi.it/brochure. pdf

[33] Cracow University of Technology webside [Online, 2014, Nov] http://www.windlab.pl/

[34] F. Pierella, P. Krogstad, L. Saetran, *Invitation to the 2012 "Blind test 2" Workshop Calculations for two wind turbines in line,* March 2012

[35] National Renewable Energy Laboratory http://wind.nrel.gov/airfoils/shapes/S826_Shape.html

[36] P. Krogstad, M. S. Adaramola, *Performance and near wake measurements of a model horizontal axis wind turbine*, Willey Online Library, 2011

[37] F. E. Jorgensen, *How to measure turbulence with hot-wire anemometers – a practical guide*, Dantec Dynamics, 2002

[38] P. Krogstad, J.A. Lund, *An experimental and numerical study of the performance of a model turbine*, Willey Online Library, 2011

[39] A.J. Wheeler, A.R. Ganji. *Introduction to engineering experimentation.* Pearson/Prentice Hall, 2004

[40] J. Bartl, F. Pierella, L. Saetran, Wake measurements behind an array of two model wind turbines, Deep-Wind Conference, Elsevier, 2012

[41] H. Schumann, F. Pierella, L. Saetran, Experimental investigation of wind turbines wakes in the wind tunnel, Deep-Wind, 2013

Appendix A – Layout of the turbines

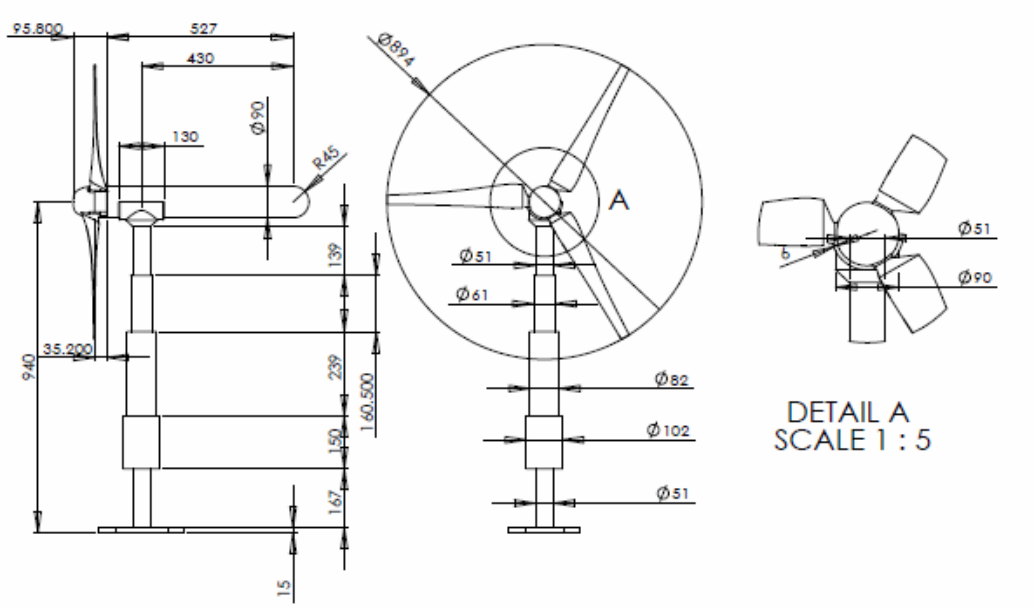

(a) Downstream Turbine, T_2

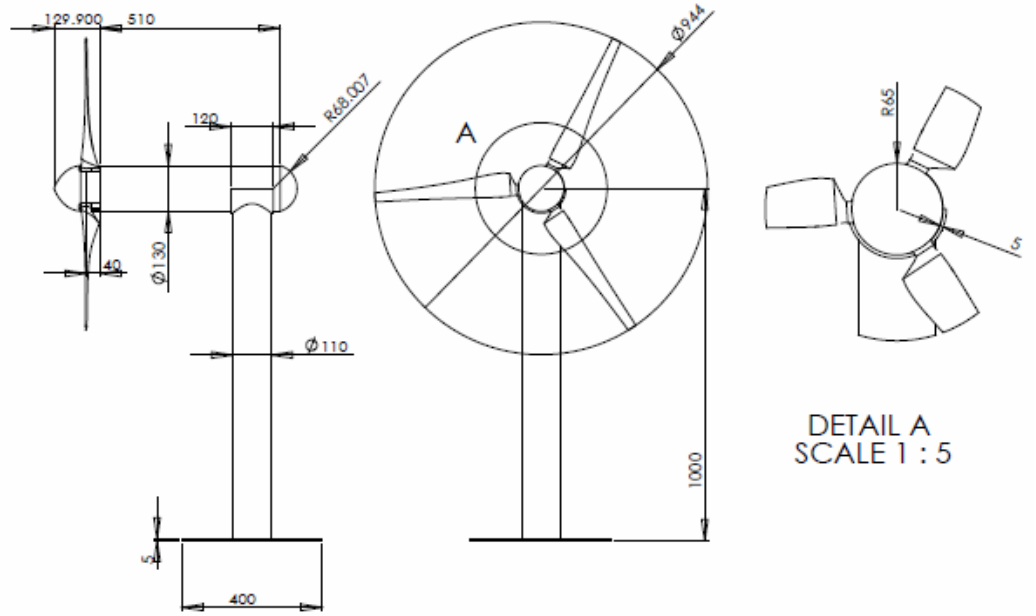

(b) Upstream Turbine, T_1